

1 **Genome sequencing and assessment of plant growth-promoting properties of a** 2 ***Serratia marcescens* strain isolated from vermicompost**

3
4 Filipe P. Matteoli^a, Hemanoel Passarelli-Araujo^a, Régis Josué A. Reis^b, Letícia O. da Rocha^b, Emanuel M.
5 de Souza^c, L. Aravind^d, Fabio L. Olivares^{b#} and Thiago M. Venancio^{1#}
6

7 ^a Laboratório de Química e Função de Proteínas e Peptídeos, Universidade Estadual do Norte Fluminense
8 Darcy Ribeiro (UENF), Rio de Janeiro, Brazil; ^b Núcleo de Desenvolvimento de Insumos Biológicos para a
9 Agricultura (NUDIBA), Universidade Estadual do Norte Fluminense Darcy Ribeiro (UENF), Rio de Janeiro,
10 Brazil. ^c Departamento de Bioquímica, Universidade Federal do Paraná (UFPR), Paraná, Brazil; ^d National
11 Center for Biotechnology Information, National Library of Medicine, National Institutes of Health,
12 Bethesda, Maryland, United States of America.
13

14
15 # Corresponding authors:

16 Fabio L. Olivares: fabioliv@uenf.br

17 Thiago M. Venancio: thiago.venancio@gmail.com
18

19 **ABSTRACT**

20
21 Plant-bacteria associations have been extensively studied for their potential in increasing crop
22 productivity in a sustainable manner. *Serratia marcescens* is a Gram-negative species found in a wide
23 range of environments, including soil. Here we describe the genome sequencing and assessment of
24 plant-growth promoting abilities of *S. marcescens* UENF-22GI (SMU), a strain isolated from mature cattle
25 manure vermicompost. *In vitro*, SMU is able to solubilize P and Zn, to produce indole compounds (likely
26 IAA), to colonize hyphae and counter the growth of two phytopathogenic fungi. Inoculation of maize
27 with SMU remarkably increased seedling growth and biomass under greenhouse conditions. The SMU
28 genome has 5 Mb, assembled in 17 scaffolds comprising 4,662 genes (4,528 are protein-coding). No
29 plasmids were identified. SMU is phylogenetically placed within a clade comprised almost exclusively of
30 environmental strains. We were able to find the genes and operons that are likely responsible for all the
31 interesting plant-growth promoting features that were experimentally described. Genes involved other
32 interesting properties that were not experimentally tested (e.g. tolerance against metal contamination)
33 were also identified. The SMU genome harbors a horizontally-transferred genomic island involved in
34 antibiotic production, antibiotic resistance, and anti-phage defense via a novel ADP-ribosyltransferase-
35 like protein and possible modification of DNA by a deazapurine base, which likely contributes to the
36 SMU competitiveness against other bacteria. Collectively, our results suggest that *S. marcescens* UENF-
37 22GI is a strong candidate to be used in the enrichment of substrates for plant growth promotion or as
38 part of bioinoculants for Agriculture.
39
40
41

42 INTRODUCTION

43 The current projections of the world population growth creates an increasing pressure for the
44 adoption of intensive farming, often resulting in reduced soil fertility, eutrophication of aquatic and
45 terrestrial environments and destruction of the biodiversity (Bhardwaj et al. 2014). Moreover,
46 conventional agriculture settings often generate large volumes of organic wastes, constituting a major
47 source of environmental pollution due to rejection or incineration (Angulo et al. 2012). Sustainable
48 strategies to minimize these problems have been investigated worldwide, particularly in developing
49 countries like Brazil, where agriculture plays a major role in the balance of trade (Olivares et al. 2017).

50 Composting and vermicomposting are widely known techniques that involve the stabilization of
51 organic materials, with a concomitant sustainable production of valuable soil amendments (Quagliotto
52 et al. 2006). Classical composting is defined as the biological decomposition of organic wastes in an
53 aerobic environment carried out by microorganisms (Sim and Wu 2010), while vermicomposting also
54 involves earthworms that promote aeration and help in waste stabilization by fragmenting the organic
55 matter and boosting microbial activity (Domínguez et al. 2003). Vermicomposting has a thermophilic
56 stage, promoted by a thermophilic bacterial community that drives the most intensive decomposition.
57 This stage is followed by a mesophilic maturation phase that is largely mediated by earthworms and
58 associated microbes (Pathma and Sakhivel 2012). Vermicomposted material holds greater amounts of
59 total phosphorus (P), micronutrients and humic acid substances than the original organic material. In
60 general, vermicomposts are considered a safe, cheap and rich source of beneficial microorganisms and
61 nutrients for plants (Hashemimajid et al. 2004). Further, bacteria isolated from vermicompost typically
62 display greater saprophytic competence than those intimately associated with plants. From a
63 biotechnological perspective, the microbial survival and activity in the absence of a host plant represent
64 an ecological advantage that can be used as a strategy to enrich substrates with nutrients, boosting
65 plant growth and development (i.e. plant substrate biofortification) (Busato et al. 2012; Busato et al.
66 2017).

67 Plants often benefit from mutualistic interactions with plant growth-promoting rhizobacteria
68 (PGPR) (Ma et al. 2016). PGPR can promote plant growth by various mechanisms, such as: 1) mitigation
69 of abiotic stresses such as metal phytotoxicity (Glick 2010), water or salinity stress (Rho et al. 2017); 2)
70 activation of defense mechanisms against phytopathogens (Hol et al. 2013); 3) directly attacking
71 pathogens (Liu et al. 2017); 4) biological nitrogen fixation (da Costa et al. 2014); 5) solubilization of
72 mineral nutrients (e.g. P and zinc, Zn) (Oteino et al. 2015); 6) production phytohormones (Ortiz-Castro et
73 al. 2009) and; 7) secretion of specific enzymes (e.g., 1-aminocyclopropane-1-carboxylate deaminase)
74 (Sarkar et al. 2017). Due to their interesting beneficial effects, there is a growing market for PGPR
75 biofertilizers (Balasubramanian and Karthickumar 2017), which are based on bacteria of various genera,
76 such as *Azospirillum*, *Bacillus* and *Azotobacter* (Bashan et al. 2014). A notable example of successful
77 application of PGPR in agriculture is the soybean (*Glycine max* L.) production in Brazil, in which the
78 development and use of an optimized consortium of different strains of *Bradyrhizobium* sp. (Souza et al.
79 2015) led to very high productivity levels at significantly lower costs due to the virtually complete
80 replacement of nitrogen fertilizers (Chang et al. 2015).

81 Knowledge of PGPR genomic content and plant interaction mechanisms has increased with the
82 progress of second-generation sequencing technologies (MacLean et al. 2009), which also allowed a
83 number of comparative genomics studies. In a large-scale comparative analyses of alpha, beta and

84 gamma-proteobacteria, Bruto et al. found no set of plant beneficial genes common to all PGPR, although
85 the presence of certain genes could reflect bacterial ecological type, such as the presence of *ppdC*
86 (involved in auxin biosynthesis) exclusively in endophytic strains of *Azospirillum* and *Bradyrhizobium*
87 (Bruto et al. 2014). *Bacillus amyloliquefaciens* subsp. *plantarum* FZB42 is a clear example of how genome
88 mining strategies can uncover the genetic basis of plant-growth promoting capacity of a PGPR (Paterson
89 et al. 2016). After promising results on auxin (Idris et al. 2007) and phytase (Makarewicz et al. 2006)
90 production *in vitro*, genome analysis also uncovered the molecular basis of how this strain exerts its
91 antifungal (Koumoutsis et al. 2004), antibacterial (Wu et al. 2015) and nematicidal activities (Liu et al.
92 2013). Another important example of genomic analysis of a PGPR is that of *Herbaspirillum seropedicae*
93 SmR1, in which genes associated with nitrogen fixation and plant colonization were elegantly
94 investigated (Pedrosa et al. 2011).

95 *Serratia marcescens* is a Gram-negative and rod-shaped bacteria that has been proposed as a
96 PGPR due to its P solubilization properties (Ben Farhat et al. 2009; Tripura et al. 2007), chitinase activity
97 (Vaikuntapu et al. 2016) and prodigiosin-mediated insect biocontrol (Suryawanshi et al. 2015). *S.*
98 *marcescens* has been described in association with several plants, such as cotton (*Gossypium hirsutum*)
99 and maize (*Zea mays*) (McInroy and Kloepper 1995), rice (*Oryza sativa*) (Gyaneshwar et al. 2001) and
100 pinus (*Pinus pinaster*) (Vicente et al. 2016). *S. marcescens* FS14 (isolated from *Atractylodes*
101 *macrocephala*) was shown to exert antagonistic effects against phytopathogenic fungi and genomic
102 sequencing revealed the presence of an interesting pattern of secretion systems (Li et al. 2015). Some *S.*
103 *marcescens* isolates have also been reported as opportunistic pathogens (Mahlen 2011) and most
104 comparative genomics studies of this species focused exclusively on its clinical relevance
105 (Moradigaravand et al. 2016). A comparative analysis of insect and clinical *S. marcescens* isolates
106 revealed a substantial genetic diversity, as supported by a relatively low intra-species average
107 nucleotide identity (ANI) of 95.1%. Further, a type II secretion system, often related to virulence
108 (Korotkov et al. 2012), was found in the clinical but not in the insect strain (Iguchi et al. 2014).

109 Here we report a comprehensive characterization of *S. marcescens* UENF-22GI (SMU), a strain
110 that has been shown to be abundant in mature cattle manure vermicompost, from where it was
111 isolated. We performed a series of *in vitro* and *in vivo* experiments that show SMU's ability to solubilize
112 P and Zn, to synthesize indole compounds (likely the auxin indole acetic acid, IAA) and to counter the
113 growth of phytopathogenic fungi. Inoculation with SMU substantially increased maize growth and
114 biomass under greenhouse conditions. Given its promising results as a PGPR, we sequenced its genome
115 and carefully identified the genetic basis of these and other important features. The SMU genome also
116 harbors an interesting horizontally-transferred genomic island involved in production of a peptide
117 antibiotic and phage resistance via modification of DNA by a deazapurine base, which probably
118 contributes to its competitiveness against other microorganisms. Further, phylogenetic reconstructions
119 placed SMU in a clade that mainly comprises non-clinical *S. marcescens* isolates. Collectively, our results
120 strongly indicate that SMU is a good candidate to be used in inoculant formulations or as part of a
121 strategy for biological enrichment of plant substrates.

122
123
124
125

126 RESULTS AND DISCUSSION

127

128 Identification of the isolate

129 During the initial characterization of abundant culturable bacteria from the mature cattle
130 vermicompost, we identified a notorious pigmented bacterium that was preliminarily characterized as a
131 *S. marcescens* by colony morphology, microscopy and 16S rRNA sequencing. This isolate was named
132 *Serratia marcescens* UENF-22GI (SMU). SMU was tested for a series of plant growth-promotion traits
133 and, given the promising results, submitted it to whole-genome sequencing and comparative analysis.

134

135 *In vitro* solubilization of P and Zn and synthesis of indole compounds by SMU

136 We explored the capacity of SMU to solubilize P and Zn *in vitro*, as the availability of these
137 elements is often a limiting factor in crop production (Mehra et al. 2017). We used the formation of a
138 halo as a positive result for the solubilization of P and Zn, which are essential nutrients for bacterial
139 growth. The halo and colony dimensions were also used to calculate a solubilization index (SI), which is a
140 useful metric to estimate the P and Zn solubilization capacities. Our results clearly show that SMU
141 solubilizes P and Zn *in vitro*, with SI values of 2.47 ± 0.22 and 2.11 ± 0.47 , respectively (Figure 1a and b).
142 We have also used a quantitative approach to measure P solubilization using two distinct inorganic P
143 sources: calcium phosphate (P-Ca) and fluorapatite rock P (P-rock). Remarkably, we found that SMU
144 increases the amount of soluble P by 12- and 13-fold with P-Ca and P-rock, respectively (Figure 1c).
145 Because acidification is a common P solubilization mechanism, we have also monitored pH variation and
146 found a striking media acidification using glucose as carbon source, from 7.0 to 3.78 and 3.54 for P-Ca
147 and P-rock, respectively (Figure 1d). Importantly, most P-solubilization screenings are conducted only
148 using Ca-P. However, in most tropical soils, P is typically associated with Fe and Al. The ability of SMU to
149 solubilize P from P-rock is important, as this P source is recommended for organic agricultural systems.
150 Hence, we propose that P-rock and SMU could be used in combination as a P-fertilization strategy for
151 tropical soils.

152 Bacterial production of phytohormones (e.g. indole-3-acetic acid, IAA, an auxin) is considered a
153 major factor in enhancing plant growth (Santoyo et al. 2016). IAA is a primary regulator of plant growth
154 and development. At least four tryptophan-dependent IAA biosynthesis pathways have been identified
155 in Bacteria: indole-3-acetamide (IAM), indole-3-acetonitrile (IAN), indole-3-pyruvic acid (IPyA) and
156 tryptamine (TAM) pathways (Duca et al. 2014; Spaepen and Vanderleyden 2011). Since the IAA
157 biosynthesis genes are also involved in the Ehrlich pathway (degradation of amino acids via
158 transamination, decarboxylation and dehydrogenation), gene presence alone is not sufficient to
159 determine IAA production. Therefore, we tested the ability of SMU to synthesize indole compounds *in*
160 *vitro* and verified that it is indeed able to produce IAA either in the presence or in the absence of Trp.
161 However, greater IAA levels were observed in the former condition (Figure 2).

162

163 Biofilm formation and biocontrol of phytopathogenic fungi

164 Many fungi colonize the rhizosphere and must cope with strong competition from soil bacteria.
165 Several of these fungi are phytopathogenic and pose serious risks to agriculture (Schwessinger et al.
166 2015). In order to assess the antifungal properties of SMU, we performed a dual growth assay and found
167 that SMU counters the growth of *F. oxysporum* and *F. solani* (Figure 3). The strategy deployed by SMU to

168 hinder fungal growth probably involves massive biofilm formation on *Fusarium* hyphae (Figure 3, Figure
169 S1), which probably facilitates the colonization and degradation of fungal cell walls. In addition, there is
170 a conspicuous delineation of the space occupied by *F. solani* by prodigiosin (Figure S1), supporting the
171 previously proposed antifungal activity of this this secondary metabolite (Duzhak et al. 2012).

172 We have also performed a time-course dual growth experiment using *F. solani* and SMU for 12
173 days, which confirmed the results described above, indicating that *F. solani* does not outcompete SMU,
174 even over a longer time period (Figure S1). Importantly, SMU did not display any obvious negative effect
175 on the growth of *Trichoderma* sp. (Figure S1), a well-known plant growth-promoting fungus. This
176 suggests that SMU and *Trichoderma* sp. are compatible and could be tested in combination on inoculant
177 formulations. Finally, the SMU ability to limit *F. solani* growth cannot be merely attributed to the
178 physical occupation of the Petri dish, as a similar effect was not observed when *H. seropedicae*, a well-
179 know PGPR, was used in the dual growth assays (Figure S1).

180

181 **SMU substantially increases growth and biomass of maize seedlings**

182 We conducted a pilot gnotobiotic experiment to evaluate whether SMU can promote plant
183 growth, which is the overall effect of the beneficial properties of a PGPR on the host plant. The
184 inoculation of plants can be performed using different methods (e.g. dipping, seed and soil inoculation)
185 (Bashan et al. 2014). We evaluated the potential of SMU in enhancing maize growth *in vivo* by applying a
186 suspension of SMU cells over maize seedlings for 10 days (Figure 4). Our results show that inoculation
187 with SMU led to substantial increases in root and shoot mass (fresh and dry weight), as well as in plant
188 height and radicular length. The biomass increment was 100 % in plant and root length, 80 % for fresh
189 root mass, 64 % for fresh shoot mass and 150 % for dry root and dry shoot mass. Previous studies have
190 shown beneficial effects of other *S. marcescens* isolates on plants, such as in the mitigation of salt stress
191 in wheat (Singh and Jha 2016) and in ginger growth promotion (Dinesh et al. 2015). Another study
192 showed that *S. marcescens* can also be useful in soil phytoremediation (Dong et al. 2014). Thus, our
193 results demonstrate that SMU promote maize growth, probably by a combination of beneficial effects.

194

195 **Genome structure and comparative analysis**

196 Given the interesting *in vitro* and *in vivo* results, we submitted the SMU genome to whole-
197 genome sequencing using an Illumina HiSeq 2500 instrument (paired-end mode, 2 x 100 bp reads).
198 Sequencing reads were processed with Trimmomatic and assembled with Velvet (see methods for
199 details). The assembled genome consisted of 17 scaffolds (length ≥ 500 bp) encompassing 5,001,184 bp,
200 with a 59.7 % GC content and an N50 of 3,077,593 bp. The genome has 4528 protein-coding genes, 84
201 and 11 tRNA and rRNA genes, respectively (Figure S2). We used BUSCO (Simao et al. 2015) to estimate
202 genome completeness and detected the complete set of 781 *Enterobacteriales* single-copy genes,
203 supporting the good quality and completeness of the assembled genome (Figure S2). No plasmids were
204 detected in the SMU genome by using plasmidSPADES and Plasmid Finder.

205 In order to understand genomic features at a species level, we computed the *S. marcescens* pan-
206 genome. A pan-genome is defined as the entire gene repertoire of a given species (Xiao et al. 2015). We
207 used 35 *S. marcescens* isolates with complete or scaffold-level genomes (Table S1). A total of 16,456
208 gene families were identified, consisting of 2,107 core genes shared by 100 % of the isolates, 7,656

209 accessory genes shared by more than one and less than 35 isolates and 57 genes unique to SMU (Figure
210 5a, Table S2). A recent study of 205 clinical strains from the United Kingdom and Ireland reported a pan-
211 genome of 13,614 genes, 3,372 core and 10,215 accessory genes (Moradigaravand et al. 2016).
212 Interestingly, despite the greater number of strains in the clinical study, the reported pan-genome is
213 smaller than that reported here, likely due to the greater diversity of the isolates in our study.

214 We performed a phylogenetic reconstruction of the strains included in the pan-genome analysis
215 using 10 single-copy core genes that were also present in the BUSCO reference set. Our phylogenetic
216 reconstructions show a good level of separation of clinical and environmental isolates (Figure 5b). We
217 also computed genome-to-genome distance using the dDDH method (Thompson et al. 2013), which
218 corroborate the structure observed in the phylogenetic tree. Interestingly, a similar partial separation of
219 pathogenic and non-pathogenic strains was also observed in *Burkholderia* and *Paraburkholderia*,
220 respectively (Eberl and Vandamme 2016). Taken together, these results indicate that phylogenetic
221 analysis can also help to assess the applicability of new candidate PGPR. Comparative genomic analysis
222 helped us identify potential genomic islands that might contribute to the competitiveness of this
223 species. In addition to the comparative genomics analysis and phylogenetic reconstructions, we also
224 carefully mined for genes potentially involved in the promotion of plant growth (Table 1). These genes
225 are grouped and discussed according to their general roles, namely: P and Zn solubilization, production
226 of indole compounds (e.g. IAA) and spermidine, biofilm formation, pathogen competition and
227 bioremediation. These findings are discussed in detail in the following sections.

228

229 **Identification and analysis of the horizontally transferred Gap1 island**

230 Our comparative analysis uncovered a remarkable region in the SMU genome that is absent in
231 most other *S. marcescens* genomes, which we named as Gap1 (Figure 6a). However, Gap1 is partially
232 conserved in the JSK296 and ATCC14041 strains (Figure 6b), which belong to the SMU phylogenetic
233 clade. Although partially eroded in several members of the clade, this result lends additional support to
234 the greater proximity of SMU to a group of environmental strains (Figure 6b). Manual analysis assisted
235 by results from IslandViewer allowed us to predict that this ~52 Kb long genomic island contains 38
236 genes. This island encodes its own integrase of the tyrosine recombinase superfamily (AK961_03610),
237 which is also encoded by several phages and bacterial mobile elements (Iyer and Aravind 2012),
238 suggesting that it supports its own genetic mobility. Genomic islands with closely related genes were
239 also detected in several distantly related proteobacteria, such as *Erwinia piriflorinigrans* CFBP 5888,
240 *Erwinia sp.* ErVv1, *Hahella sp.* CCB-MM4, *Enterobacter sp.* T1-1 and [*Polyangium*] *brachysporum*,
241 suggesting that fitness-conferring determinants carried by this island might have facilitated their
242 dissemination by HGT. Further, the closest cognates of at least 15 genes (AK961_03495 : AK961_03565)
243 in this island are found in *Erwinia* species raising the possibility of a relatively recent genetic exchange
244 event involving *Serratia* and *Erwinia*.

245 We next investigated the island to identify genes potentially functioning as fitness determinants
246 which could explain this wide dissemination. At the 5' flank of the island are two genes respectively
247 encoding a JAB domain protein of the RadC family and ArdB domain (AK961_03485, AK961_03490).
248 These genes were recently identified as part of a system of proteins that enable mobile elements such
249 as conjugative transposons and plasmids to evade restriction by host defense systems (Iyer et al. 2017).
250 The core of the island contains an operon, which is shared with the related islands that we detected in

251 the above-stated bacteria, encoding the system predicted to synthesize a non-ribosomal peptide. The
252 two largest genes (AK961_03515, AK961_03520) of this operon code for two giant multidomain non-
253 ribosomal-peptide synthetases (NRPS), together with 4 predicted AMPylating domains that charge acyl
254 groups and 3 condensation domains that ligate charged amino acids to form a peptide bond.
255 Additionally, the operon contains a further gene for a standalone AMPylating enzyme and one for a
256 thioesterase of the α/β -hydrolase fold (AK961_03545, AK961_03550). The last enzyme has been shown
257 to be required for generation of a cyclic peptide in several NRPS systems (Schneider and Marahiel 1998).
258 Thus, the system encoded by this island has the potential to synthesize tetra- or penta-peptide skeleton
259 with a possibly cyclic structure. Notably, the region also encodes a GNAT acetyltransferase
260 (AK961_03495) that might either modify this peptide or confer auto-resistance against its toxicity. Also
261 in this operon is a gene for a pol- β superfamily nucleotidyltransferase (AK961_03530), which might
262 modify the peptide generated by the NRPS by the addition of a nucleotide, or regulate its
263 production/secretion by nucleotidylation of one of the components of the system. The said operon
264 codes for a predicted peptide transporter of the MFS superfamily that probably facilitates the export of
265 the synthesized peptide out of the cell. Taken together, we interpret this NRPS system and associated
266 proteins are generating an anti-microbial peptide.

267 We also found this island to encode a protein belonging to a previously unknown family of the
268 ADP-ribosyltransferase (ART) fold (AK961_03540) (Aravind et al. 2015). Using sequence profile searches
269 and profile-profile comparisons we showed that this novel family also includes the Pfam (“Domain of
270 unknown function”) DUF4433 and the abortive phage infection protein AbiGi. Members of the ART
271 superfamily utilize NAD^+ to either transfer it to target substrates (e.g. proteins) or degrade NAD^+ . Given
272 the relationship to the AbiGi proteins, we predict that this protein might also play a role in anti-phage
273 defense by means of its ADP-ribosyltransferase activity targeted either at self or viral proteins. In a
274 similar vein, we also found an ATPase of the ABC superfamily (AK961_03575) that is related to AbiEii,
275 another abortive infection protein involved in anti-phage systems. More remarkably, the gene encoding
276 this protein is also part of an operon coding for a KAP NTPase (AK961_03580) and another protein
277 (AK961_03585), which are a version of an anti-phage system centered on these two proteins (Aravind et
278 al. 2004). Of these the proteins, AK961_03585 is predicted to function as a novel DNA transglycosylase
279 that is predicted to incorporate a modified base into DNA, which is likely to be a deazaguanine acquired
280 from the queuine biosynthesis pathway (Iyer et al. 2013).

281 Taken together, this island codes for multiple distinct fitness-promoting systems: one predicted
282 to synthesize a potential antimicrobial peptide that could be deployed against competing organisms in
283 compost. Further, it also encodes a beta-lactam amidase (AK961_03565) that could likely defend SMU
284 against certain beta-lactams (e.g. penicillin) produced by competing bacteria. The further set of genes is
285 likely to confer resistance against certain bacteriophages and potentially enhance the fitness of this
286 strain relative to other *Serratia* lacking the island.

287

288 **Phosphorus and zinc solubilization genes**

289 As discussed above, in tropical environments, P is mostly present in poorly soluble mineral
290 phosphates that are not readily available for plant uptake (An and Moe 2016). Microbial conversion of
291 insoluble mineral P forms into soluble ionic phosphate (H_2PO_4^-) is a key mechanism of increasing the P
292 availability (Alori et al. 2017). Further, the production and secretion of a variety of low molecular weight

293 acids constitute a major strategy to solubilize not only P (An and Moe 2016), but also Zn (Solanki et al.
294 2016). Among these substances, gluconic acid, produced by three oxidation reactions carried out by
295 membrane-bound periplasmic proteins (Krishnaraj and Goldstein 2001), is typically the most prominent.

296 The SMU genome harbors a number of genes involved in the production of gluconic acid from
297 glucose (Table 1), which starts with the oxidation of glucose by a membrane-bound, periplasmic
298 pyrroloquinoline-quinone (PQQ)-dependent glucose dehydrogenase (GDH; AK961_10840). The
299 intermediate glucono-1,5-lactone is hydrolyzed to gluconate by a gluconolactonase (AK961_17880) and
300 oxidized by 2-gluconate dehydrogenase (AK961_08395) to 2-ketogluconate, which is oxidized to 2-5-
301 diketo gluconate by 2-keto-gluconate dehydrogenase, an enzymatic complex comprising a small
302 (AK961_17580), a large (AK961_17575) and a cytochrome (AK961_17570) subunits (as in *Gluconobacter*
303 *oxydans*, accession AB985494), encoded in the same operon. Gluconic acid synthesis requires the PQQ
304 cofactor (Duine 1991), which is produced by proteins encoded by the *pqqBCDEF* operon. Importantly,
305 this operon is fully conserved in the SMU genome (genes AK961_07090 : AK961_07110) (Table 1; Figure
306 S3). The SMU genome also has a conserved *pstABCS* operon (AK961_21130 : AK961_21145) (Table 1;
307 Figure S2b), which encodes a phosphate-specific transport system. Finally, current data indicate that Zn
308 solubilization is largely carried out by the same genes involved in the solubilization of inorganic P
309 (Intorne et al. 2009). Therefore, based on genomic data and *in vitro* evidence, we hypothesize that SMU
310 solubilizes P and Zn through soil acidification.

311

312 **Tolerance against metal toxicity**

313 Successful soil bacteria often have to tolerate metal contamination, which can involve different
314 strategies (Das et al. 2016). In addition, PGPR can alleviate the impact of heavy metals on plants by
315 reduction, oxidation, methylation and conversion to less toxic forms (Hassan et al. 2017). We found a
316 number of genes related to these roles in the SMU genome (Table 1): arsenate reductase
317 (AK961_01055), *arsRBC* (AK961_03990, AK961_03995, AK961_04000), copper resistance protein
318 (AK961_01905, AK961_01915, AK961_09290), *cusRS* (AK961_11430, AK961_11425), chromate
319 transporter *ChrA* (AK961_07435, AK961_07440) chromate reductase (AK961_21085) and *czcD*
320 (AK961_12615). Although this list is likely incomplete due to the wide diversity of reactions and
321 pathways involved in these tolerance pathways, our findings are in line with those from a recently
322 sequenced genome of a *S. marcescens* strain that alleviates cadmium stress in plants (Khan et al. 2017).
323 Notably, a gene from the Gap1 island (AK961_03595) codes for a member of the YfeE-like transporter
324 family, which transport chelated Fe/Mn and could potentially play a role in alleviating toxicity from
325 these transition metals.

326

327 **IAA, spermidine biosynthesis and phenolic compound transport**

328 We searched for IAA biosynthesis pathways in the SMU genome and found the *ipdC* gene (Table
329 1). This gene encodes a key enzyme responsible for the conversion of indole-3-pyruvate in indole-3-
330 acetaldehyde, a critical step of the IPyA pathway. Disruption of *ipdC* dramatically decreases IAA
331 production in *A. brasilense* (Malhotra and Srivastava 2008). In addition, we have also identified two
332 putative auxin efflux carrier genes (AK961_00655, AK961_12310) (Table 1), suggesting that SMU also
333 exports IAA. These results indicate that the IPyA pathway is active in SMU. Other IAA biosynthesis

334 pathways were only partially identified and the genes pertaining to these pathways are also part of
335 other processes. Hence, activity of alternative pathways in SMU warrants further investigation.

336 In addition to IAA, we have also found the *speAB* (AK961_18130, AK961_18125) and *speDE*
337 (AK961_18275, AK961_18270) operons, which are involved in spermidine biosynthesis (Table 1).
338 Polyamines (e.g. spermidines) are essential for eukaryotic cells viability and have been correlated with
339 lateral root development, pathogen resistance and alleviation of oxidative, osmotic and acidic stresses
340 (Xie et al. 2014). Therefore, spermidine production by SMU may constitute an additional mechanism
341 involved in plant-growth promotion.

342 Several plants produce phenolic compounds, which are part of their defense system and are also
343 regulators of their own growth. Interestingly, the Gap1 island codes for a 4-hydroxybenzoate
344 transporter (AK961_03620), which is closely related to cognate transporters from other plant-associated
345 bacteria, such as *Pantoea ananatis*, *Erwinia amylovorans*, *Pseudomonas putida*, and *Dickeya* species.
346 This suggests that this transporter might play a role in the plant-bacterium interaction via phenolic
347 compounds such as benzoate, as has been proposed for certain *Xanthomonas* species (Wang et al.
348 2015).

349

350 **Biofilm formation and biocontrol of phytopathogenic fungi**

351 Bacterial biofilms are multicellular communities entrapped within an extracellular polymeric
352 matrix (Flemming et al. 2016) that are essential for survival, microbe-microbe interactions and root
353 colonization (Kasim et al. 2016). We found several biofilm related genes in the SMU genome (Table 1),
354 such as *pgaABCD* (AK961_01650 : AK961_01665) (Figure S3). This operon is responsible for the
355 production of poly- β -1,6-N-acetyl-D-glucosamine (PGA), which is associated with surface attachment,
356 intercellular adhesion and biofilm formation in several species (Echeverez et al. 2017).

357 Cellulose is the fundamental component of plant cell walls and the most abundant biopolymer
358 in nature. Cellulose biosynthesis has been also described in a broad range of bacteria and a variety of
359 bacterial cellulose synthase operons are known (Römling and Galperin 2015). In proteobacteria,
360 cellulose biosynthesis is mainly carried out by the *bcsABZC* and *bcsEFG* operons, along with the *bcsQ* and
361 *bcsR* genes, described as the *E. coli*-like *bcs* operon (Krasteva et al. 2017). The *bcsABZC* (AK961_20475,
362 AK961_20470, AK961_20465, AK961_20460) and *bcsEFG* (AK961_20490, AK961_20495, AK961_20500)
363 operons are proximal to each other in the SMU genome, although in opposite strands (Figure S3). The
364 opposite orientation of these operons is also observed in others *S. marcescens* strains (e.g. WW4, B3R3
365 and UMH8), and might be related to the transcriptional regulation of biofilm synthesis in *S. marcescens*.
366 Further, there are two regulatory genes upstream to the *bcsABZC* operon: *bcsQ* (AK961_20480) and
367 *bcsR* (AK961_20485). These regulatory genes were also reported to be required for cellulose synthesis
368 and subcellular localization of an active biosynthesis apparatus at the bacterial cell pole in γ -
369 proteobacteria (Le Quéré and Ghigo 2009). We have also found the *adrA* gene (AK961_13115), which
370 encodes a diguanylate cyclase that synthesizes cyclic dimeric GMP, which binds to the BcsA and
371 activates cellulose production (Cowles et al. 2016). BcsA has two cytoplasmic domains and
372 transmembrane segments, while BcsB is located in the periplasm, anchored to the membrane; together
373 they form the BcsAB complex, which function as a channel for the addition of new residues to the
374 nascent glucan molecule (Römling and Galperin 2015). BcsC is an outer membrane pore (Whitney and
375 Howell 2013) and BcsZ is an endoglucanase that may be involved in the alignment of β -glucans prior to

376 export (Castiblanco and Sundin 2016), or act as negative regulator of cellulose production (Ahmad et al.
377 2016). The *bcsEFG* operon is also necessary for optimal cellulose synthesis (Fang et al. 2014) and its
378 deletion disrupted cellulose production (Serra et al. 2013).

379

380 **Fungi biocontrol, prodigiosin production and resistance to antimicrobial compounds**

381 Chitinases are central to the catabolism of chitin (i.e. poly β -(1 \rightarrow 4)-N-acetyl-D-glucosamine),
382 constituting a route by which bacteria can access a rich source of nutrients (Paspaliari et al. 2017).
383 Chitinases break chitin into soluble oligosaccharides that can be transported into the periplasm via a
384 chitoporin channel, where they are further processed into mono- and di-saccharides that are
385 transported to the cytoplasm (Hayes et al. 2017). Because of the severe impact of phytopathogenic
386 fungi in agriculture (Santamarina et al. 2017), chitinases have received increased attention by the
387 scientific community as a biocontrol mechanism deployed by several bacteria, including *S. marcescens*
388 (Vaikuntapu et al. 2016). We found 4 chitinases in the SMU genome (Table 1); to further classify them
389 we performed BLASTp searches on the Swissprot database. AK961_20530 shares 99 % identity with
390 chitinase A (accession: P07254), AK961_01270 shares 100 % identity with chitinase B (accession:
391 P11797), AK961_12935 shares 29 % identity and 93 % coverage with chitinase D (accession: P27050) and
392 AK961_05475 shares 31 % identity and 88 % coverage with chitinase A1 (accession: P20533). We have
393 also found other chitin metabolism genes in SMU, namely AK961_01260 and AK961_12890, which
394 encode a chitin-binding protein and a chitobiase, respectively. Bacterial chitinases have been reported
395 to compromise fungal spore integrity and generate germ tube abnormalities (Pandey et al. 2016).
396 Further, ChiA promotes the degradation of mycelia of several phytopathogenic fungi, including
397 *Fusarium*, *Acremonium* and *Alternaria* species (Medina-de la Rosa et al. 2016). Chitinase applications are
398 not restricted to fungal biocontrol and can also be deployed for bioremediation and bioconversion of
399 chitin wastes, as well as part of an insect biocontrol strategies (Hamid et al. 2013).

400 As part of the arms race between microorganisms, several *Fusarium* species produce fusaric
401 acid, a mycotoxin reported to be toxic to some microorganisms, such as *P. fluorescens* (Crutcher et al.
402 2017). Interestingly, SMU has a gene that encodes a fusaric acid resistance protein (AK961_08005),
403 which may render SMU resistant to this toxin, indirectly boosting its fungicidal activity.

404 We have also found a widely-conserved operon comprising genes involved in the biosynthesis of
405 prodigiosin (i.e. the *pig* operon), the notorious red pigment observed in several *Serratia* isolates (Mahlen
406 2011). The *pig* operon in the SMU genome comprises 14 genes (Table 1, Figure S3) arranged in a
407 structure that resembles the *pig* operon from *S. marcescens* ATCC274 (also an environmental isolate)
408 (Harris et al. 2004). Prodigiosin is most commonly found in environmental *S. marcescens* isolates and has
409 been proposed to suppress growth of various fungi (Duzhak et al. 2012), bacteria (Danevčič et al. 2016),
410 protozoans (Genes et al. 2011) and even viruses (Zhou et al. 2016). It has been recently suggested that
411 prodigiosin has affinity for the lipid bilayer of the plasmatic membrane, causing outer membrane
412 damage (Darshan and Manonmani 2016). Although the mechanistic details of the prodigiosin antifungal
413 and antibacterial activities remain largely unclear, our findings on the dual growth experiments indicate
414 that that the *pig* operon is active in SMU and that prodigiosin delineates the growth area of *F. solani*
415 (Figure 3, Figure S1).

416 *Streptomyces* species are ubiquitous in the soil and notable for the production of several
417 antimicrobials (Barka et al. 2016). Therefore, the presence of genes conferring resistance against these

418 antimicrobials is a desirable feature of a successful PGPR. SMU produces several resistance proteins
419 against *Streptomyces* antimicrobials such as bicyclomycin (AK961_03740, AK961_14040, AK961_02590),
420 fosmidomycin (AK961_13395) and kasugamycin (AK961_16235). In addition, SMU also exhibits a type 6
421 secretion system (T6SS) (AK961_04125-AK961_04210) that can mediate interbacterial antagonistic
422 interactions (Russell et al. 2014; Zhang et al. 2012).

423

424 **CONCLUDING REMARKS**

425 In this study we assessed the plant growth-promoting properties of SMU using *in vitro* biochemical
426 assays and *in vivo* experiments in greenhouse conditions. Specifically, we found that SMU is able to: 1)
427 solubilize inorganic P and Zn; 2) produce indole compounds; 3) counter the growth of two
428 phytopathogenic *Fusarium* species by a combination of physical (i.e. biofilm formation) and biochemical
429 (e.g. prodigiosin, chitinase) properties and; 4) substantially increase growth and biomass of maize
430 seedlings. Given these interesting properties, we sequenced the SMU genome and mapped the genes
431 that are likely responsible for these traits. Interestingly, the SMU genome also harbors a mobile genomic
432 island comprising 38 genes that were horizontally transferred. This region codes for a NRPS systems and
433 other proteins predicted to confer fitness advantage by various mechanisms, including DNA modification
434 and anti-phage defenses. Phylogenetic analysis show that SMU groups within a clade comprised almost
435 exclusively of non-clinical isolates. Together with the absence of plasmids and synthesis of prodigiosin,
436 more frequent in environmental isolates, we hypothesize that SMU is non-pathogenic. However, basic
437 safety issues must be addressed before biotechnological applications can be envisaged. Collectively, our
438 results add important information regarding *S. marcescens* plant growth-promoting abilities that can
439 inspire future applications in inoculant formulations.

440

441 **MATERIALS AND METHODS**

442 **Vermicompost maturation**

443 Mature vermicompost was produced with dry cattle manure as substrate inside a 150 L cement
444 ring. Humidity was kept at 60-70%, by weekly watering and mixing. After 1 month, earthworms (*Eisenia*
445 *foetida*) were introduced at the rate of 5 kg·m³. After 4 months, earthworms were removed and the
446 vermicompost was placed in plastic bags and stored at 25°. At the final maturation stage, the chemical
447 composition of the substrate (in g·kg⁻¹) was as follows: total nitrogen (1.9 ± 0.4); total carbon (22.99 ±
448 3.3); P₂O₅ (6.97 ± 1.4); C/N ratio of 13.8 ± 0.4 and pH (H₂O) = 6.6 ± 0.18.

449

450 **Bacterial isolation and DNA purification**

451 Serial dilutions were performed on a solution prepared by adding 10 g of vermicompost in 90
452 mL of saline (8.5 g·L⁻¹ NaCl), followed by shaking for 60 minutes. Next, 1 mL of the initial dilution (10⁻¹)
453 was added to a new tube containing 9 mL of saline (10⁻²), and successively until 10⁻⁷ dilution. Then, 100
454 µL of the final dilutions from 10⁻⁵ to 10⁻⁷ were taken and spread on plates containing solid Nutrient Broth
455 (NB) with 8 g·L⁻¹ of NB and 15 g·L⁻¹ of agar in 1 L of distilled water. After incubation at 30 °C for 7 days,
456 different colony types could be identified and, for purification, individual colonies were transferred to
457 Petri plates with Dygs solid media (Döbereiner et al. 1995) containing 2 g·L⁻¹ of glucose, 2 g·L⁻¹ of malic
458 acid, 1.5 g·L⁻¹ of bacteriological peptone, 2 g·L⁻¹ of yeast extract, 0.5 g·L⁻¹ of K₂HPO₄, 0.5 g·L⁻¹ of
459 MgSO₄·7H₂O, 1.5 g·L⁻¹ of glutamic acid and 15 g·L⁻¹ of agar, adjusted to pH 6.0; these supplies were

460 acquired from Vetec (São Paulo, Brazil). From the last dilution (10^{-7}) and after the isolation and
461 purification on Dygs solid medium, a pink-to-red, circular, pulvinate elevation, punctiform and smooth
462 surface bacterial colony was selected. Phase contrast microscopy revealed the presence of Gram-
463 negative, rod-shaped and non-motile cells. This distinctive isolate, named UENF-22GI, was stored in 16
464 mL glass flask containing 5 mL of Nutrient Broth solid medium covered with mineral oil and later grown
465 in liquid Dygs medium under rotatory shaker at 150 rpm and 30 °C for 36 h to perform *in vitro* and *in*
466 *vivo* assays. Total DNA of UENF-22GI was extracted using QIAamp® DNA Mini Kit (QIAGEN GmbH, Hilden,
467 Germany). DNA quantification and quality assessment were performed using an Agilent Bioanalyzer
468 2100 instrument (Agilent, California, USA).

469

470 **Phosphorus and zinc solubilization**

471 Bacterial inocula were grown for 36 h on liquid Dygs media at 150 rpm and 30 °C until
472 approximately 10^8 cells.mL⁻¹ ($O.D_{540nm} = 1.0$) (Döbereiner et al. 1995). To carry out a qualitative P
473 solubilization assay, 10 µL of the bacterial suspension were added to petri dishes containing 10 g·L⁻¹ of
474 glucose, 5 g·L⁻¹ of ammonium chloride (NH₄Cl), 1 g·L⁻¹ of sodium chloride, 1 g·L⁻¹ of magnesium sulfate
475 heptahydrate (MgSO₄·7H₂O), 15 g·L⁻¹ of agar in 1 L of distilled water at pH 7.0, and incubated at 30 °C for
476 7 days. Two mineral P sources were tested: calcium phosphate Ca₃(PO₄)₂ (P-Ca) and fluorapatite rock
477 phosphate Ca₁₀(PO₄)₆F₂ (P-rock), both at 1 g·L⁻¹. Positive P solubilization phenotypes were based on halo
478 formation around bacterial colonies and results were expressed in the form of a Solubilization Index (SI),
479 calculated as the halo diameter (d1) divided by the colony diameter (d2). The SI values can be used to
480 classify the solubilization ability of a strain as low (SI < 2), intermediate (2 < SI < 4) and high (SI > 4)
481 (Marra et al. 2015).

482 Quantitative P solubilization assays were also performed. 50 µL bacterial suspensions in Dygs
483 liquid medium were transferred to 30 mL test tubes containing Pikovskaya liquid medium at pH 7.0,
484 supplemented with P-Ca or P-rock at 1 g·L⁻¹. The assay was carried out in orbital shaker at 150 rpm at 30
485 °C. After 7 days growth, a 5 mL aliquot was harvested and centrifuged at 3200 rpm for 15 min. The
486 supernatant was used to determine the pH and to quantify soluble P levels by the colorimetric
487 ammonium molybdate method ($\lambda = 600$ nm). Results were expressed in mg of PO₄²⁻·L⁻¹.

488 Zn solubilization was evaluated using 10 µL aliquots taken from the bacterial suspension and
489 dropped onto petri dishes containing solid media (Saravanan et al. 2007) constituted of 10 g·L⁻¹ of
490 glucose, 1 g·L⁻¹ of ammonium sulfate ((NH₄)₂SO₄), 0.2 g·L⁻¹ of potassium chloride (KCl), 0.1 g·L⁻¹ of
491 dipotassium phosphate (K₂HPO₄), 0.2 g·L⁻¹ of magnesium sulfate heptahydrate, 1.0 g·L⁻¹ of zinc oxide
492 (ZnO), 15 g·L⁻¹ agar, 1 L distilled water; the medium was incubated for 7 days at 30 °C. Zn solubilization
493 was also assessed by halo formation around bacterial colonies. Both, Zn and P solubilization assays were
494 carried out in triplicates.

495

496 **Production of indole compounds**

497 To quantify the production of indole compounds, previously grown bacteria were transferred to
498 glass tubes containing 5 mL of Dygs medium with or without tryptophan addition (100 mg·L⁻¹), followed
499 by 72 h incubation in the dark, at 30 °C and 150 rpm. To evaluate indole synthesis (Sarwar and Kremer
500 1995), 150 µL of grown bacteria were transferred to microplates and 100 µL of Salkowski reagent, which
501 was prepared by diluting 1 mL of an iron trichloride hexahydrated (FeCl₃·6H₂O) aqueous solution at 92.5

502 g·L⁻¹ in 50 mL of perchloric acid (HClO₄) 350 g·L⁻¹ in water. The plate was incubated for 30 min in the dark
503 and samples analyzed at 492 nm on a UV mini 1240 spectrophotometer (Shimadzu, Japan). This assay
504 was conducted in triplicate.

505

506 ***In vitro* dual culture assays**

507 *In vitro* bacterial-fungal dual culture assays were performed in 9 cm diameter Petri dishes
508 containing Potato Dextrose Agar solid medium. A 5 mm diameter disk taken from the edge of actively
509 growing hyphae of *F. solani* and *F. oxysporum* were inoculated at the center of each Petri dish.
510 Suspensions of SMU were spotted in four equidistant quadrant points to the inoculated fungal disk.
511 Control treatments (without SMU) were conducted in parallel to monitor fungal growth. Treatments
512 were carried out for 10 days and three independent replicates were performed. In addition, time-course
513 dual culture experiments were also performed for 12 days with SMU and *F. solani* or *Trichoderma* sp., a
514 plant growth-promoting fungus. We have also tested *F. solani* in dual growth assays with *H. seropedicae*
515 HRC54, a well-known PGPR without known anti-fungal properties. Samples from the transition zones
516 between fungi structures and spotted bacteria were mounted on glass slide and coverslip, observed
517 under phase-contrast inverted optical microscope Zeiss Axio 10 Observer A1 and photodocumented
518 with an AxioCam MRC 5 digital camera. For the time-course assays between *F. solani* and SMU (1 -12
519 days of growth), bacterial inocula were spotted in three equidistant quadrant points to the inoculated
520 fungal disk.

521

522 ***In vivo* plant-growth promotion assays**

523 Maize (*Zea mays* var. UENF/506-11) seeds were surface-disinfected using ethanol 70 % for 30
524 seconds, followed by a wash with 5 % sodium hypochlorite (NaClO) for 20 min. Next, seeds were washed
525 5 times with sterile distilled water under stirring for 3 minutes and transferred to petri dishes containing
526 1.5 % solidified agar for pre-germination for 4 days. Seedlings with 2.0 to 2.5 cm radicle length were
527 carefully transferred under flow chamber to glass tubes of 2 cm diameter and 20 cm height containing
528 10 g of sterilized vermiculite (one seed per tube). Meanwhile, the bacterial inoculum was prepared by
529 growth in Dygs liquid media for 36 h, at 30 °C and 120 rpm. Inoculation was performed by application of
530 1 mL of the SMU suspension (10⁸ cells·mL⁻¹) over the seedlings. Plants inoculated with 1 mL of sterile
531 Dygs medium were used as negative controls. The assay was carried out under laboratory conditions
532 with average temperature at 30 °C and 12 h of light/dark photoperiod. After 10 days, plants were
533 collected and the following biometric measurements were registered: height (cm), total radicular length
534 (cm), fresh root mass (mg), fresh shoot mass (mg), dry root mass (mg) and dry shoot mass (mg). This
535 assay was performed in four replicates. Statistical analyses were performed using the SAEG software
536 (Universidade Federal de Viçosa, Brazil) and obtained means were compared with the Tukey test.

537

538 **Genome sequencing and assembly**

539 Paired-end libraries were prepared with the TruSeq Nano DNA LT Library Prep (Illumina) and
540 sequenced on a HiSeq 2500 instrument at the Life Sciences Core Facility (LaCTAD; UNICAMP, Campinas,
541 Brazil). The quality of the sequencing reads (2 x 100bp) was checked with FastQC 0.11.5
542 (<https://www.bioinformatics.babraham.ac.uk/projects/fastqc/>). Quality filtering was performed with
543 Trimmomatic 0.35 (Bolger et al. 2014) and only reads with average quality greater than 30 were used.

544 The UENF-22GI genome was assembled with Velvet 1.2.10 (Zerbino and Birney 2008), with the aid of
545 VelvetOptimiser 2.2.6 (Gladman and Seemann 2008). Scaffolding was performed with SSPACE 3.0 with
546 default parameters (Boetzer et al. 2011). QUASt 4.0 (Gurevich et al. 2013) was used to assess general
547 assembly statistics. Genome completeness was assessed with BUSCO 3.0 (Simao et al. 2015), using the
548 *Enterobacteriales* dataset as reference.

549

550 **Genome annotation and phylogenetic analysis**

551 The assembled genome was annotated with the NCBI Prokaryotic Genome Annotation Pipeline
552 (Tatusova et al. 2016). Some annotations were manually improved with primary literature information
553 and specific searches using BLAST (Altschul et al. 1997) and Kegg Orthology And Links Annotation
554 (BlastKOALA) (Kanehisa et al. 2016). The presence of plasmids was assessed with plasmidSPAdes 3.10
555 (Antipov et al. 2016) and PlasmidFinder 1.3 (Carattoli et al. 2014). Genes and operons involved in
556 antibiotic and secondary metabolism were predicted using antiSMASH 4.0 (Blin et al. 2017). The SMU
557 genome was deposited on Genbank under the BioProject PRJNA290503.

558 Whole genome comparisons were done using BRIG 0.95 (Alikhan et al. 2011) and synteny was
559 assessed using Synima v 1.0 (Farrer 2017). Horizontal gene transfer regions were inferred with
560 IslandViewer4 (Bertelli et al. 2017) followed by manual adjustments. Pan-genome analysis was
561 performed with BPGA 1.3.0 (Chaudhari et al. 2016). Phylogenetic reconstructions were carried out using
562 the predicted proteins of 10 core housekeeping genes that were also present in the BUSCO's reference
563 dataset. Protein sequences were aligned using MUSCLE 3.8.31 (Edgar 2004) and evolutionary model
564 selected with protest 3.4.2 (Darriba et al. 2011). Maximum-likelihood phylogenetic reconstructions were
565 performed using RAxML 8.2.10 (Stamatakis 2014), with the Le and Gascuel model (Le and Gascuel 2008),
566 gamma correction, SH local support and 1000 bootstrap replicates. Genomic distance patterns were
567 computed with the digital DNA:DNA hybridization (dDDH) (Auch et al. 2010). The resulting phylogenetic
568 tree and dDDH values were integrated and rendered in iTOL 3 (Letunic and Bork 2016).

569

570 **ACKNOWLEDGEMENTS**

571 This work was supported by Fundação Carlos Chagas Filho de Amparo à Pesquisa do Estado do Rio de
572 Janeiro, Conselho Nacional de Desenvolvimento Científico e Tecnológico (CNPq) and Coordenação de
573 Aperfeiçoamento de Pessoal de Nível Superior (CAPES). We would like to thank the staff of the Life
574 Sciences Core Facility (LaCTAD) of UNICAMP for library preparation and genome sequencing. We also
575 thank Prof. Valdirene Gomes (UENF) for kindly providing the *Fusarium* strains and to Francisnei Pedrosa
576 for helping in figure preparation.

577

578 **REFERENCES**

579

580 Ahmad I, Rouf SF, Sun L, Cimdins A, Shafeeq S, Guyon S, Schottkowski M, Rhen M, Römling U (2016) BcsZ
581 inhibits biofilm phenotypes and promotes virulence by blocking cellulose production in
582 *Salmonella enterica* serovar Typhimurium. *Microbial cell factories* 15(1):177
583 Alikhan N-F, Petty NK, Zakour NLB, Beatson SA (2011) BLAST Ring Image Generator (BRIG): simple
584 prokaryote genome comparisons. *BMC genomics* 12(1):402

- 585 Alori ET, Glick BR, Babalola OO (2017) Microbial Phosphorus Solubilization and Its Potential for Use in
586 Sustainable Agriculture. *Frontiers in microbiology* 8
- 587 Altschul SF, Madden TL, Schäffer AA, Zhang J, Zhang Z, Miller W, Lipman DJ (1997) Gapped BLAST and
588 PSI-BLAST: a new generation of protein database search programs. *Nucleic acids research*
589 25(17):3389-3402
- 590 An R, Moe LA (2016) Regulation of Pyrroloquinoline Quinone-Dependent Glucose Dehydrogenase
591 Activity in the Model Rhizosphere-Dwelling Bacterium *Pseudomonas putida* KT2440. *Appl*
592 *Environ Microbiol* 82(16):4955-64 doi:10.1128/AEM.00813-16
- 593 Angulo J, Mahecha L, Yepes SA, Yepes AM, Bustamante G, Jaramillo H, Valencia E, Villamil T, Gallo J
594 (2012) Quantitative and nutritional characterization of fruit and vegetable waste from
595 marketplace: A potential use as bovine feedstuff? *J Environ Manage* 95:S203-S209
596 doi:10.1016/j.jenvman.2010.09.022
- 597 Antipov D, Hartwick N, Shen M, Raiko M, Lapidus A, Pevzner P (2016) plasmidSPAdes: assembling
598 plasmids from whole genome sequencing data. bioRxiv:048942
- 599 Aravind L, Iyer LM, Leipe DD, Koonin EV (2004) A novel family of P-loop NTPases with an unusual
600 phyletic distribution and transmembrane segments inserted within the NTPase domain.
601 *Genome biology* 5(5):R30 doi:10.1186/gb-2004-5-5-r30
- 602 Aravind L, Zhang D, de Souza RF, Anand S, Iyer LM (2015) The natural history of ADP-ribosyltransferases
603 and the ADP-ribosylation system. *Current topics in microbiology and immunology* 384:3-32
604 doi:10.1007/82_2014_414
- 605 Auch AF, Jan M, Klenk H-P, Göker M (2010) Digital DNA-DNA hybridization for microbial species
606 delineation by means of genome-to-genome sequence comparison. *Standards in Genomic*
607 *Sciences* 2(1):117
- 608 Balasubramanian P, Karthickumar P (2017) Biofertilizers and Biopesticides: A Holistic Approach for
609 Sustainable Agriculture. *Sustainable Utilization of Natural Resources*:255
- 610 Barka EA, Vatsa P, Sanchez L, Gaveau-Vaillant N, Jacquard C, Klenk H-P, Clément C, Ouhdouch Y, van
611 Wezel GP (2016) Taxonomy, physiology, and natural products of Actinobacteria. *Microbiology*
612 *and Molecular Biology Reviews* 80(1):1-43
- 613 Bashan Y, de-Bashan LE, Prabhu S, Hernandez J-P (2014) Advances in plant growth-promoting bacterial
614 inoculant technology: formulations and practical perspectives (1998–2013). *Plant and Soil*
615 378(1-2):1-33
- 616 Ben Farhat M, Farhat A, Bejar W, Kammoun R, Bouchaala K, Fourati A, Antoun H, Bejar S, Chouayekh H
617 (2009) Characterization of the mineral phosphate solubilizing activity of *Serratia marcescens*
618 CTM 50650 isolated from the phosphate mine of Gafsa. *Archives of microbiology* 191(11):815-24
619 doi:10.1007/s00203-009-0513-8
- 620 Bertelli C, Laird MR, Williams KP, Group SFURC, Lau BY, Hoad G, Winsor GL, Brinkman FS (2017)
621 IslandViewer 4: expanded prediction of genomic islands for larger-scale datasets. *Nucleic acids*
622 *research* 45(W1):W30-W35
- 623 Bhardwaj D, Ansari MW, Sahoo RK, Tuteja N (2014) Biofertilizers function as key player in sustainable
624 agriculture by improving soil fertility, plant tolerance and crop productivity. *Microbial cell*
625 *factories* 13(1):66

- 626 Blin K, Wolf T, Chevrette MG, Lu X, Schwalen CJ, Kautsar SA, Suarez Duran HG, De Los Santos EL, Kim HU,
627 Nave M (2017) antiSMASH 4.0—improvements in chemistry prediction and gene cluster
628 boundary identification. *Nucleic acids research* 45(W1):W36-W41
- 629 Boetzer M, Henkel CV, Jansen HJ, Butler D, Pirovano W (2011) Scaffolding pre-assembled contigs using
630 SSPACE. *Bioinformatics* 27(4):578-579
- 631 Bolger AM, Lohse M, Usadel B (2014) Trimmomatic: a flexible trimmer for Illumina sequence data.
632 *Bioinformatics*:btu170
- 633 Bruto M, Prigent-Combaret C, Muller D, Moenne-Loccoz Y (2014) Analysis of genes contributing to plant-
634 beneficial functions in Plant Growth-Promoting Rhizobacteria and related Proteobacteria.
635 *Scientific reports* 4:6261 doi:10.1038/srep06261
- 636 Busato JG, Lima LS, Aguiar NO, Canellas LP, Olivares FL (2012) Changes in labile phosphorus forms during
637 maturation of vermicompost enriched with phosphorus-solubilizing and diazotrophic bacteria.
638 *Bioresource technology* 110:390-5 doi:10.1016/j.biortech.2012.01.126
- 639 Busato JG, Zandonadi DB, Mol AR, Souza RS, Aguiar KP, Junior FB, Olivares FL (2017) Compost
640 biofortification with diazotrophic and P-solubilizing bacteria improves maturation process and P
641 availability. *Journal of the science of food and agriculture* 97(3):949-955 doi:10.1002/jsfa.7819
- 642 Carattoli A, Zankari E, García-Fernández A, Larsen MV, Lund O, Villa L, Aarestrup FM, Hasman H (2014) In
643 silico detection and typing of plasmids using PlasmidFinder and plasmid multilocus sequence
644 typing. *Antimicrobial agents and chemotherapy* 58(7):3895-3903
- 645 Castiblanco LF, Sundin GW (2016) Cellulose production, activated by cyclic di-GMP through BcsA and
646 BcsZ, is a virulence factor and an essential determinant of the three-dimensional architectures
647 of biofilms formed by *Erwinia amylovora* Ea1189. *Molecular Plant Pathology*
- 648 Chang W-S, Lee H-I, Hungria M (2015) Soybean production in the Americas Principles of Plant-Microbe
649 Interactions. Springer, pp 393-400
- 650 Chaudhari NM, Gupta VK, Dutta C (2016) BPGA- an ultra-fast pan-genome analysis pipeline. *Scientific*
651 *reports* 6:24373 doi:10.1038/srep24373
- 652 Cowles KN, Willis DK, Engel TN, Jones JB, Barak JD (2016) Diguanylate cyclases AdrA and STM1987
653 regulate *Salmonella enterica* exopolysaccharide production during plant colonization in an
654 environment-dependent manner. *Applied and environmental microbiology* 82(4):1237-1248
- 655 Crutcher FK, Puckhaber LS, Stipanovic RD, Bell AA, Nichols RL, Lawrence KS, Liu J (2017) Microbial
656 Resistance Mechanisms to the Antibiotic and Phytotoxin Fusaric Acid. *Journal of chemical*
657 *ecology* 43(10):996-1006
- 658 da Costa PB, Granada CE, Ambrosini A, Moreira F, de Souza R, dos Passos JF, Arruda L, Passaglia LM
659 (2014) A model to explain plant growth promotion traits: a multivariate analysis of 2,211
660 bacterial isolates. *PLoS One* 9(12):e116020 doi:10.1371/journal.pone.0116020
- 661 Danevčič T, Vežjak MB, Tabor M, Zorec M, Stopar D (2016) Prodigiosin induces autolysins in actively
662 grown *Bacillus subtilis* cells. *Frontiers in microbiology* 7
- 663 Darriba D, Taboada GL, Doallo R, Posada D (2011) ProtTest 3: fast selection of best-fit models of protein
664 evolution. *Bioinformatics* 27(8):1164-1165
- 665 Darshan N, Manonmani H (2016) Prodigiosin inhibits motility and activates bacterial cell death revealing
666 molecular biomarkers of programmed cell death. *AMB Express* 6(1):50

- 667 Das S, Dash HR, Chakraborty J (2016) Genetic basis and importance of metal resistant genes in bacteria
668 for bioremediation of contaminated environments with toxic metal pollutants. *Applied*
669 *microbiology and biotechnology* 100(7):2967-2984
- 670 Dinesh R, Anandaraj M, Kumar A, Bini YK, Subila KP, Aravind R (2015) Isolation, characterization, and
671 evaluation of multi-trait plant growth promoting rhizobacteria for their growth promoting and
672 disease suppressing effects on ginger. *Microbiological research* 173:34-43
- 673 Döbereiner J, Baldani VLCD, Baldani JI (1995) Como isolar e identificar bactérias diazotróficas de plantas
674 não-leguminosas. *Embrapa Agrobiologia*
- 675 Domínguez J, Parmelee RW, Edwards CA (2003) Interactions between *Eisenia andrei* (Oligochaeta) and
676 nematode populations during vermicomposting. *Pedobiologia* 47(1):53-60 doi:10.1078/0031-
677 4056-00169
- 678 Dong R, Gu L, Guo C, Xun F, Liu J (2014) Effect of PGPR *Serratia marcescens* BC-3 and AMF *Glomus*
679 *intraradices* on phytoremediation of petroleum contaminated soil. *Ecotoxicology* 23(4):674-80
680 doi:10.1007/s10646-014-1200-3
- 681 Duca D, Lorv J, Patten CL, Rose D, Glick BR (2014) Indole-3-acetic acid in plant–microbe interactions.
682 *Antonie Van Leeuwenhoek* 106(1):85-125
- 683 Duine JA (1991) Quinoproteins: enzymes containing the quinonoid cofactor pyrroloquinoline quinone,
684 topaquinone or tryptophan-tryptophan quinone. *The FEBS Journal* 200(2):271-284
- 685 Duzhak A, Panfilova Z, Duzhak T, Vasyunina E, Shternshis M (2012) Role of prodigiosin and chitinases in
686 antagonistic activity of the bacterium *Serratia marcescens* against the fungus *Didymella*
687 *applanata*. *Biochemistry (Moscow)* 77(8):910-916
- 688 Eberl L, Vandamme P (2016) Members of the genus *Burkholderia*: good and bad guys. *F1000Research* 5
- 689 Echeverz M, García B, Sabalza A, Valle J, Gabaldón T, Solano C, Lasa I (2017) Lack of the PGA
690 exopolysaccharide in *Salmonella* as an adaptive trait for survival in the host. *PLoS genetics*
691 13(5):e1006816
- 692 Edgar RC (2004) MUSCLE: multiple sequence alignment with high accuracy and high throughput. *Nucleic*
693 *acids research* 32(5):1792-1797
- 694 Fang X, Ahmad I, Blanka A, Schotchkowski M, Cimmins A, Galperin MY, Römling U, Gomelsky M (2014) GIL,
695 a new c-di-GMP-binding protein domain involved in regulation of cellulose synthesis in
696 enterobacteria. *Molecular microbiology* 93(3):439-452
- 697 Farrer RA (2017) Synima: a Synteny imaging tool for annotated genome assemblies. *BMC bioinformatics*
698 18(1):507
- 699 Flemming H-C, Wingender J, Szewzyk U, Steinberg P, Rice SA, Kjelleberg S (2016) Biofilms: an emergent
700 form of bacterial life. *Nature Reviews Microbiology* 14(9):563
- 701 Genes C, Baquero E, Echeverri F, Maya JD, Triana O (2011) Mitochondrial dysfunction in *Trypanosoma*
702 *cruzi*: the role of *Serratia marcescens* prodigiosin in the alternative treatment of Chagas disease.
703 *Parasites & vectors* 4(1):66
- 704 Gladman S, Seemann T (2008) VelvetOptimiser.
- 705 Glick BR (2010) Using soil bacteria to facilitate phytoremediation. *Biotechnol Adv* 28(3):367-74
706 doi:10.1016/j.biotechadv.2010.02.001
- 707 Gurevich A, Saveliev V, Vyahhi N, Tesler G (2013) QUASt: quality assessment tool for genome
708 assemblies. *Bioinformatics* 29(8):1072-5 doi:10.1093/bioinformatics/btt086

- 709 Gyaneshwar P, James EK, Mathan N, Reddy PM, Reinhold-Hurek B, Ladha JK (2001) Endophytic
710 colonization of rice by a diazotrophic strain of *Serratia marcescens*. *Journal of bacteriology*
711 183(8):2634-45 doi:10.1128/JB.183.8.2634-2645.2001
- 712 Hamid R, Khan MA, Ahmad M, Ahmad MM, Abdin MZ, Musarrat J, Javed S (2013) Chitinases: an update.
713 *Journal of pharmacy & bioallied sciences* 5(1):21
- 714 Harris AK, Williamson NR, Slater H, Cox A, Abbasi S, Foulds I, Simonsen HT, Leeper FJ, Salmond GP (2004)
715 The *Serratia* gene cluster encoding biosynthesis of the red antibiotic, prodigiosin, shows species-
716 and strain-dependent genome context variation. *Microbiology* 150(11):3547-3560
- 717 Hashemimajd K, Kalbasi M, Golchin A, Shariatmadari H (2004) Comparison of vermicompost and
718 composts as potting media for growth of tomatoes. *Journal of plant nutrition* 27(6):1107-1123
- 719 Hassan TU, Bano A, Naz I (2017) Alleviation of heavy metals toxicity by the application of plant growth
720 promoting rhizobacteria and effects on wheat grown in saline sodic field. *International journal*
721 *of phytoremediation* 19(6):522-529
- 722 Hayes CA, Dalia TN, Dalia AB (2017) Systematic genetic dissection of chitin degradation and uptake in
723 *Vibrio cholerae*. *Environmental Microbiology*
- 724 Hol WH, Bezemer TM, Biere A (2013) Getting the ecology into interactions between plants and the plant
725 growth-promoting bacterium *Pseudomonas fluorescens*. *Front Plant Sci* 4:81
726 doi:10.3389/fpls.2013.00081
- 727 Idris EE, Iglesias DJ, Talon M, Borriss R (2007) Tryptophan-dependent production of indole-3-acetic acid
728 (IAA) affects level of plant growth promotion by *Bacillus amyloliquefaciens* FZB42. *Molecular*
729 *plant-microbe interactions* 20(6):619-626
- 730 Iguchi A, Nagaya Y, Pradel E, Ooka T, Ogura Y, Katsura K, Kurokawa K, Oshima K, Hattori M, Parkhill J
731 (2014) Genome evolution and plasticity of *Serratia marcescens*, an important multidrug-
732 resistant nosocomial pathogen. *Genome biology and evolution* 6(8):2096-2110
- 733 Intorne AC, de Oliveira MVV, Lima ML, da Silva JF, Olivares FL, de Souza Filho GA (2009) Identification
734 and characterization of *Gluconacetobacter diazotrophicus* mutants defective in the
735 solubilization of phosphorus and zinc. *Archives of microbiology* 191(5):477-483
- 736 Iyer LM, Aravind L (2012) ALOG domains: provenance of plant homeotic and developmental regulators
737 from the DNA-binding domain of a novel class of DIRS1-type retroposons. *Biology direct* 7:39
738 doi:10.1186/1745-6150-7-39
- 739 Iyer LM, Burroughs AM, Anand S, de Souza RF, Aravind L (2017) Polyvalent Proteins, a Pervasive Theme
740 in the Intergenomic Biological Conflicts of Bacteriophages and Conjugative Elements. *Journal of*
741 *bacteriology* 199(15) doi:10.1128/JB.00245-17
- 742 Iyer LM, Zhang D, Burroughs AM, Aravind L (2013) Computational identification of novel biochemical
743 systems involved in oxidation, glycosylation and other complex modifications of bases in DNA.
744 *Nucleic acids research* 41(16):7635-55 doi:10.1093/nar/gkt573
- 745 Kanehisa M, Sato Y, Morishima K (2016) BlastKOALA and GhostKOALA: KEGG tools for functional
746 characterization of genome and metagenome sequences. *Journal of molecular biology*
747 428(4):726-731
- 748 Kasim WA, Gaafar RM, Abou-Ali RM, Omar MN, Hewait HM (2016) Effect of biofilm forming plant
749 growth promoting rhizobacteria on salinity tolerance in barley. *Annals of Agricultural Sciences*
750 61(2):217-227 doi:10.1016/j.aos.2016.07.003

- 751 Khan AR, Park G-S, Asaf S, Hong S-J, Jung BK, Shin J-H (2017) Complete genome analysis of *Serratia*
752 *marcescens* RSC-14: A plant growth-promoting bacterium that alleviates cadmium stress in host
753 plants. *PLoS one* 12(2):e0171534
- 754 Korotkov KV, Sandkvist M, Hol WG (2012) The type II secretion system: biogenesis, molecular
755 architecture and mechanism. *Nature Reviews Microbiology* 10(5):336-351
- 756 Koumoutsis A, Chen X-H, Henne A, Liesegang H, Hitzeroth G, Franke P, Vater J, Borriss R (2004) Structural
757 and functional characterization of gene clusters directing nonribosomal synthesis of bioactive
758 cyclic lipopeptides in *Bacillus amyloliquefaciens* strain FZB42. *Journal of bacteriology*
759 186(4):1084-1096
- 760 Krasteva PV, Bernal-Bayard J, Travier L, Martin FA, Kaminski P-A, Karimova G, Fronzes R, Ghigo J-M
761 (2017) Insights into the structure and assembly of a bacterial cellulose secretion system. *Nature*
762 *communications* 8(1):2065
- 763 Krishnaraj P, Goldstein A (2001) Cloning of a *Serratia marcescens* DNA fragment that induces
764 quinoprotein glucose dehydrogenase-mediated gluconic acid production in *Escherichia coli* in
765 the presence of stationary phase *Serratia marcescens*. *FEMS microbiology letters* 205(2):215-
766 220
- 767 Le Qu er  B, Ghigo JM (2009) BcsQ is an essential component of the *Escherichia coli* cellulose
768 biosynthesis apparatus that localizes at the bacterial cell pole. *Mol Microbiol* 72(3):724-740
- 769 Le SQ, Gascuel O (2008) An improved general amino acid replacement matrix. *Molecular biology and*
770 *evolution* 25(7):1307-1320
- 771 Letunic I, Bork P (2016) Interactive tree of life (iTOL) v3: an online tool for the display and annotation of
772 phylogenetic and other trees. *Nucleic acids research* 44(W1):W242-W245
- 773 Li P, Kwok AH, Jiang J, Ran T, Xu D, Wang W, Leung FC (2015) Comparative genome analyses of *Serratia*
774 *marcescens* FS14 reveals its high antagonistic potential. *PLoS One* 10(4):e0123061
775 doi:10.1371/journal.pone.0123061
- 776 Liu K, Newman M, McInroy JA, Hu C-H, Kloepper JW (2017) Selection and assessment of plant growth-
777 promoting rhizobacteria for biological control of multiple plant diseases. *Phytopathology*
778 107(8):928-936
- 779 Liu Z, Budiharjo A, Wang P, Shi H, Fang J, Borriss R, Zhang K, Huang X (2013) The highly modified
780 microcin peptide plantazolicin is associated with nematicidal activity of *Bacillus*
781 *amyloliquefaciens* FZB42. *Applied microbiology and biotechnology* 97(23):10081-10090
- 782 Ma Y, Oliveira RS, Freitas H, Zhang C (2016) Biochemical and Molecular Mechanisms of Plant-Microbe-
783 Metal Interactions: Relevance for Phytoremediation. *Front Plant Sci* 7:918
784 doi:10.3389/fpls.2016.00918
- 785 MacLean D, Jones JD, Studholme DJ (2009) Application of 'next-generation' sequencing technologies to
786 microbial genetics. *Nature reviews Microbiology* 7(4):287
- 787 Mahlen SD (2011) *Serratia* infections: from military experiments to current practice. *Clinical*
788 *microbiology reviews* 24(4):755-791
- 789 Makarewicz O, Dubrac S, Msadek T, Borriss R (2006) Dual role of the PhoP~ P response regulator:
790 *Bacillus amyloliquefaciens* FZB45 phytase gene transcription is directed by positive and negative
791 interactions with the phyC promoter. *Journal of bacteriology* 188(19):6953-6965

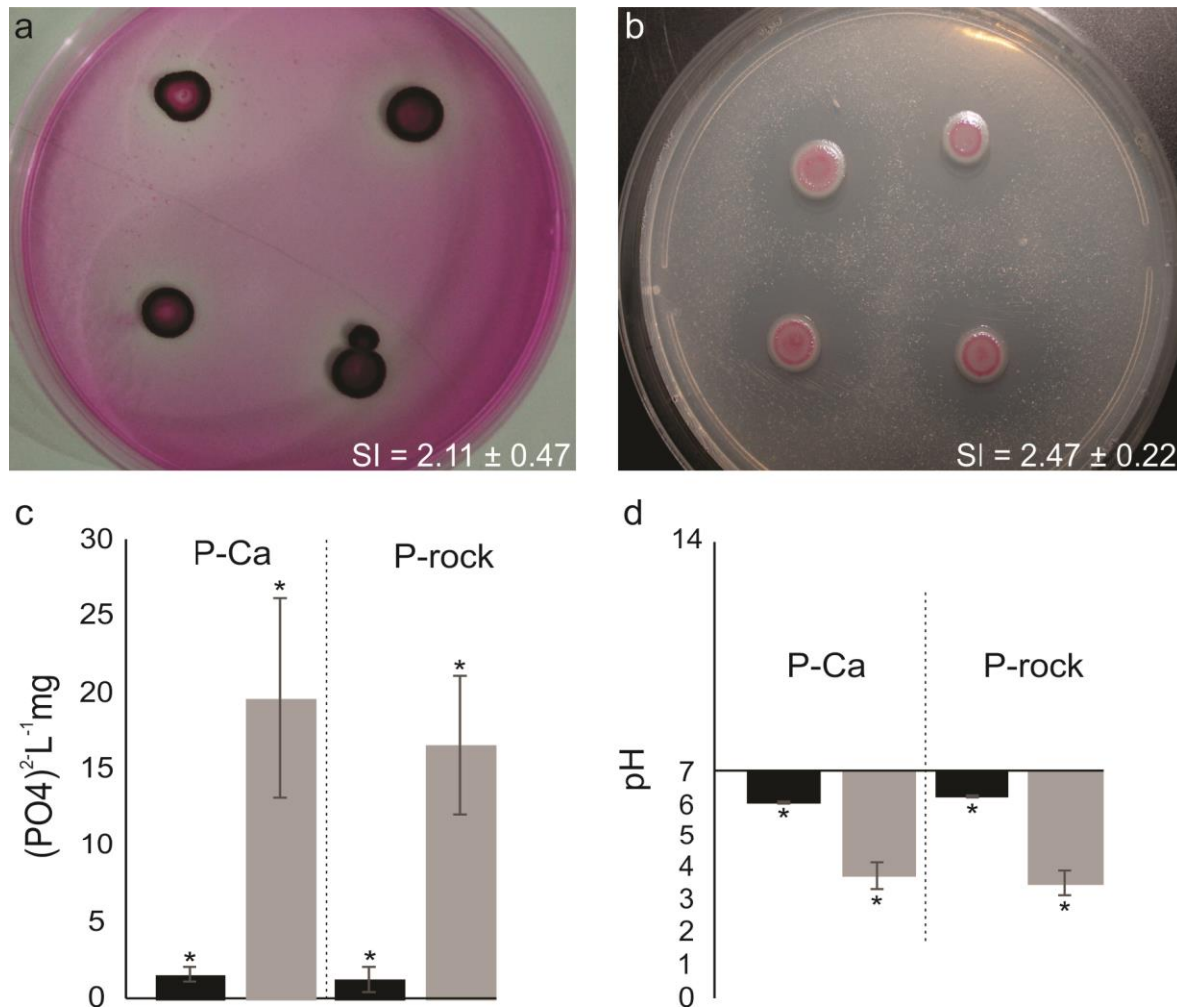
- 792 Malhotra M, Srivastava S (2008) An ipdC gene knock-out of *Azospirillum brasilense* strain SM and its
793 implications on indole-3-acetic acid biosynthesis and plant growth promotion. *Antonie Van*
794 *Leeuwenhoek* 93(4):425-433
- 795 Marra LM, Oliveira-Longatti SMd, Soares CR, Lima JMd, Olivares FL, Moreira F (2015) Initial pH of
796 medium affects organic acids production but do not affect phosphate solubilization. *Brazilian*
797 *Journal of Microbiology* 46(2):367-375
- 798 McInroy JA, Kloepper JW (1995) Survey of indigenous bacterial endophytes from cotton and sweet corn.
799 *Plant and soil* 173(2):337-342
- 800 Medina-de la Rosa G, López-Reyes L, Carcaño-Montiel MG, López-Olguín JF, Hernández-Espinosa MÁ,
801 Rivera-Tapia JA (2016) Rhizosphere bacteria of maize with chitinolytic activity and its potential in
802 the control of phytopathogenic fungi. *Archives of Phytopathology and Plant Protection* 49(11-
803 12):310-321
- 804 Mehra P, Pandey BK, Giri J (2017) Improvement in phosphate acquisition and utilization by a secretory
805 purple acid phosphatase (OsPAP21b) in rice. *Plant Biotechnology Journal*
- 806 Moradigaravand D, Boinett CJ, Martin V, Peacock SJ, Parkhill J (2016) Recent independent emergence of
807 multiple multidrug-resistant *Serratia marcescens* clones within the United Kingdom and Ireland.
808 *Genome research* 26(8):1101-1109
- 809 Olivares FL, Busato JG, Paula AM, Lima LS, Aguiar NO, Canellas LP (2017) Plant growth promoting
810 bacteria and humic substances: crop promotion and mechanisms of action. *Chemical and*
811 *Biological Technologies in Agriculture* 4(1):30
- 812 Ortíz-Castro R, Contreras-Cornejo HA, Macías-Rodríguez L, López-Bucio J (2009) The role of microbial
813 signals in plant growth and development. *Plant signaling & behavior* 4(8):701-712
- 814 Oteino N, Lally RD, Kiwanuka S, Lloyd A, Ryan D, Germaine KJ, Dowling DN (2015) Plant growth
815 promotion induced by phosphate solubilizing endophytic *Pseudomonas* isolates. *Frontiers in*
816 *microbiology* 6
- 817 Pandey A, Negi S, Soccol CR (2016) Current developments in biotechnology and bioengineering:
818 Production, isolation and purification of industrial products. Elsevier
- 819 Paspaliari DK, Kastbjerg VG, Ingmer H, Popowska M, Larsen MH (2017) Chitinase expression in *Listeria*
820 *monocytogenes* is influenced by lmo0327, which encodes an internalin-like protein. *Applied and*
821 *environmental microbiology* 83(22):e01283-17
- 822 Paterson J, Jahanshah G, Li Y, Wang Q, Mehnaz S, Gross H (2016) The contribution of genome mining
823 strategies to the understanding of active principles of PGPR strains. *FEMS microbiology ecology*
824 93(3):fiw249
- 825 Pathma J, Sakthivel N (2012) Microbial diversity of vermicompost bacteria that exhibit useful agricultural
826 traits and waste management potential. *SpringerPlus* 1(1):26
- 827 Pedrosa FO, Monteiro RA, Wasseem R, Cruz LM, Ayub RA, Colauto NB, Fernandez MA, Fungaro MHP,
828 Grisard EC, Hungria M (2011) Genome of *Herbaspirillum seropedicae* strain SmR1, a specialized
829 diazotrophic endophyte of tropical grasses. *PLoS Genet* 7(5):e1002064
- 830 Quagliotto P, Montoneri E, Tambone F, Adani F, Gobetto R, Viscardi G (2006) Chemicals from wastes:
831 compost-derived humic acid-like matter as surfactant. *Environmental science & technology*
832 40(5):1686-1692

- 833 Rho H, Hsieh M, Kandel SL, Cantillo J, Doty SL, Kim S-H (2017) Do Endophytes Promote Growth of Host
834 Plants Under Stress? A Meta-Analysis on Plant Stress Mitigation by Endophytes. *Microbial*
835 *ecology*:1-12
- 836 Römmling U, Galperin MY (2015) Bacterial cellulose biosynthesis: diversity of operons, subunits, products,
837 and functions. *Trends in microbiology* 23(9):545-557
- 838 Russell AB, Peterson SB, Mougous JD (2014) Type VI secretion system effectors: poisons with a purpose.
839 *Nature reviews microbiology* 12(2):137
- 840 Santamarina M, Ibáñez M, Marqués M, Roselló J, Giménez S, Blázquez M (2017) Bioactivity of essential
841 oils in phytopathogenic and post-harvest fungi control. *Natural product research* 31(22):2675-
842 2679
- 843 Santoyo G, Moreno-Hagelsieb G, del Carmen Orozco-Mosqueda M, Glick BR (2016) Plant growth-
844 promoting bacterial endophytes. *Microbiological research* 183:92-99
- 845 Saravanan VS, Madhaiyan M, Thangaraju M (2007) Solubilization of zinc compounds by the diazotrophic,
846 plant growth promoting bacterium *Gluconacetobacter diazotrophicus*. *Chemosphere*
847 66(9):1794-8 doi:10.1016/j.chemosphere.2006.07.067
- 848 Sarkar A, Ghosh PK, Pramanik K, Mitra S, Soren T, Pandey S, Mondal MH, Maiti TK (2017) A halotolerant
849 *Enterobacter* sp. displaying ACC deaminase activity promotes rice seedling growth under salt
850 stress. *Research in microbiology*
- 851 Sarwar M, Kremer R (1995) Determination of bacterially derived auxins using a microplate method.
852 *Letters in applied microbiology* 20(5):282-285
- 853 Schneider A, Marahiel MA (1998) Genetic evidence for a role of thioesterase domains, integrated in or
854 associated with peptide synthetases, in non-ribosomal peptide biosynthesis in *Bacillus subtilis*.
855 *Archives of microbiology* 169(5):404-10
- 856 Schwessinger B, Bart R, Krasileva KV, Coaker G (2015) Focus issue on plant immunity: from model
857 systems to crop species. *Frontiers in plant science* 6
- 858 Serra DO, Richter AM, Hengge R (2013) Cellulose as an architectural element in spatially structured
859 *Escherichia coli* biofilms. *Journal of bacteriology* 195(24):5540-5554
- 860 Sim EY, Wu TY (2010) The potential reuse of biodegradable municipal solid wastes (MSW) as feedstocks
861 in vermicomposting. *Journal of the science of food and agriculture* 90(13):2153-62
862 doi:10.1002/jsfa.4127
- 863 Simao FA, Waterhouse RM, Ioannidis P, Kriventseva EV, Zdobnov EM (2015) BUSCO: assessing genome
864 assembly and annotation completeness with single-copy orthologs. *Bioinformatics* 31(19):3210-
865 2 doi:10.1093/bioinformatics/btv351
- 866 Singh RP, Jha PN (2016) The Multifarious PGPR *Serratia marcescens* CDP-13 Augments Induced Systemic
867 Resistance and Enhanced Salinity Tolerance of Wheat (*Triticum aestivum* L.). *PLoS One*
868 11(6):e0155026 doi:10.1371/journal.pone.0155026
- 869 Solanki M, Didwania N, Nandal V (2016) Potential of Zinc Solubilizing Bacterial Inoculants in Fodder
870 Crops. *momentum*
- 871 Souza Rd, Ambrosini A, Passaglia LM (2015) Plant growth-promoting bacteria as inoculants in
872 agricultural soils. *Genetics and molecular biology* 38(4):401-419
- 873 Spaepen S, Vanderleyden J (2011) Auxin and plant-microbe interactions. *Cold Spring Harb Perspect Biol*
874 3(4) doi:10.1101/cshperspect.a001438

- 875 Stamatakis A (2014) RAxML version 8: a tool for phylogenetic analysis and post-analysis of large
876 phylogenies. *Bioinformatics* 30(9):1312-1313
- 877 Suryawanshi RK, Patil CD, Borase HP, Narkhede CP, Salunke BK, Patil SV (2015) Mosquito larvicidal and
878 pupaecidal potential of prodigiosin from *Serratia marcescens* and understanding its mechanism
879 of action. *Pesticide biochemistry and physiology* 123:49-55
- 880 Tatusova T, DiCuccio M, Badretdin A, Chetvernin V, Nawrocki EP, Zaslavsky L, Lomsadze A, Pruitt KD,
881 Borodovsky M, Ostell J (2016) NCBI prokaryotic genome annotation pipeline. *Nucleic acids
882 research* 44(14):6614-24 doi:10.1093/nar/gkw569
- 883 Thompson CC, Chimetto L, Edwards RA, Swings J, Stackebrandt E, Thompson FL (2013) Microbial
884 genomic taxonomy. *BMC genomics* 14(1):913
- 885 Tripura C, Sashidhar B, Podile AR (2007) Ethyl methanesulfonate mutagenesis-enhanced mineral
886 phosphate solubilization by groundnut-associated *Serratia marcescens* GPS-5. *Curr Microbiol
887* 54(2):79-84 doi:10.1007/s00284-005-0334-1
- 888 Vaikuntapu PR, Rambabu S, Madhuprakash J, Podile AR (2016) A new chitinase-D from a plant growth
889 promoting *Serratia marcescens* GPS5 for enzymatic conversion of chitin. *Bioresource technology*
890 220:200-7 doi:10.1016/j.biortech.2016.08.055
- 891 Vicente CS, Nascimento FX, Barbosa P, Ke H-M, Tsai IJ, Hirao T, Cock PJ, Kikuchi T, Hasegawa K, Mota M
892 (2016) Evidence for an Opportunistic and Endophytic Lifestyle of the Bursaphelenchus
893 xylophilus-Associated Bacteria *Serratia marcescens* PWN146 Isolated from Wilting Pinus
894 pinaster. *Microbial ecology* 72(3):669-681
- 895 Wang JY, Zhou L, Chen B, Sun S, Zhang W, Li M, Tang H, Jiang BL, Tang JL, He YW (2015) A functional 4-
896 hydroxybenzoate degradation pathway in the phytopathogen *Xanthomonas campestris* is
897 required for full pathogenicity. *Scientific reports* 5:18456 doi:10.1038/srep18456
- 898 Whitney J, Howell P (2013) Synthase-dependent exopolysaccharide secretion in Gram-negative bacteria.
899 *Trends in microbiology* 21(2):63-72
- 900 Wu L, Wu H, Chen L, Yu X, Borriss R, Gao X (2015) Difficidin and bacilysin from *Bacillus amyloliquefaciens*
901 FZB42 have antibacterial activity against *Xanthomonas oryzae* rice pathogens. *Scientific reports*
902 5
- 903 Xiao J, Zhang Z, Wu J, Yu J (2015) A brief review of software tools for pangenomics. *Genomics
904 Proteomics Bioinformatics* 13(1):73-6 doi:10.1016/j.gpb.2015.01.007
- 905 Xie SS, Wu HJ, Zang HY, Wu LM, Zhu QQ, Gao XW (2014) Plant growth promotion by spermidine-
906 producing *Bacillus subtilis* OKB105. *Mol Plant Microbe Interact* 27(7):655-63 doi:10.1094/MPMI-
907 01-14-0010-R
- 908 Zerbino DR, Birney E (2008) Velvet: algorithms for de novo short read assembly using de Bruijn graphs.
909 *Genome Res* 18(5):821-9 doi:10.1101/gr.074492.107
- 910 Zhang D, de Souza RF, Anantharaman V, Iyer LM, Aravind L (2012) Polymorphic toxin systems:
911 Comprehensive characterization of trafficking modes, processing, mechanisms of action,
912 immunity and ecology using comparative genomics. *Biology direct* 7:18 doi:10.1186/1745-6150-
913 7-18
- 914 Zhou W, Zeng C, Liu R, Chen J, Li R, Wang X, Bai W, Liu X, Xiang T, Zhang L (2016) Antiviral activity and
915 specific modes of action of bacterial prodigiosin against *Bombyx mori* nucleopolyhedrovirus in
916 vitro. *Applied microbiology and biotechnology* 100(9):3979-3988

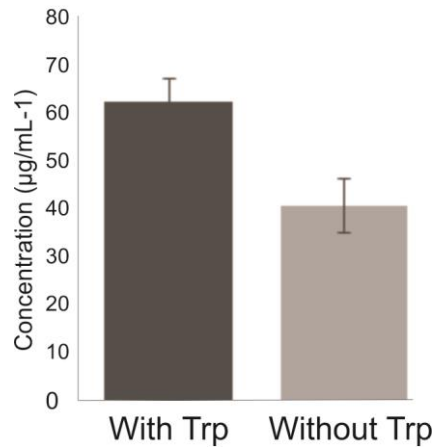
917 **FIGURES**

918



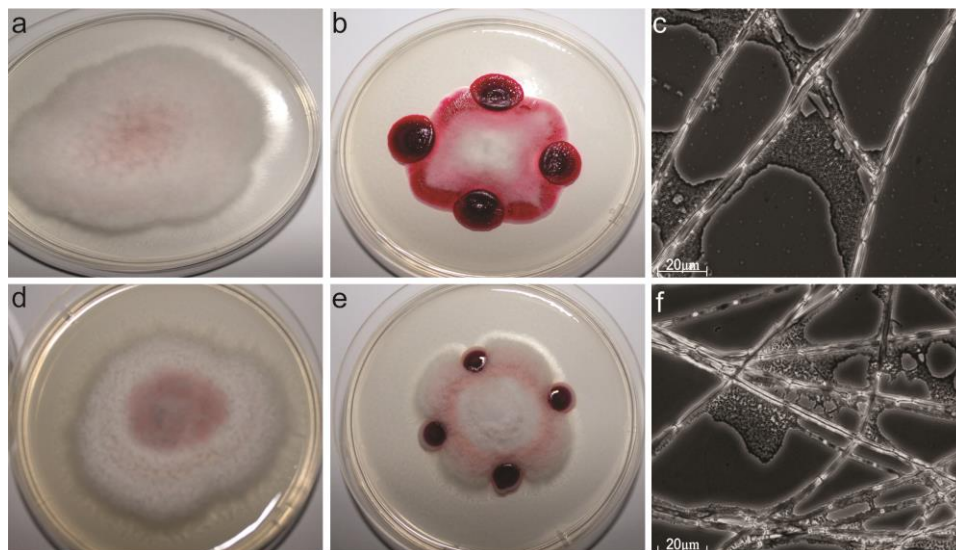
919
920

921 **Figure 1:** Phosphorus (a) and zinc (b) solubilization assays. Qualitative P and Zn solubilization assays
922 were carried out with $\text{Ca}_3(\text{PO}_4)_2$ (P-Ca) and ZnO as substrates, respectively. Halo formation around
923 growing colonies was considered a positive result for solubilization. These results were used to compute
924 the solubilization index (SI), which is the halo diameter divided by the colony diameter. Quantitative P
925 solubilization assays were also performed using P-Ca or fluorapatite rock phosphate (P-rock) in the
926 absence (black bars) or presence (gray bars) of SMU (c). pH variation in the culture media in the absence
927 (black bars) or presence (gray bars) of SMU, indicating that P solubilization is probably driven by
928 acidification (d).
929



930
931
932
933
934
935
936
937
938

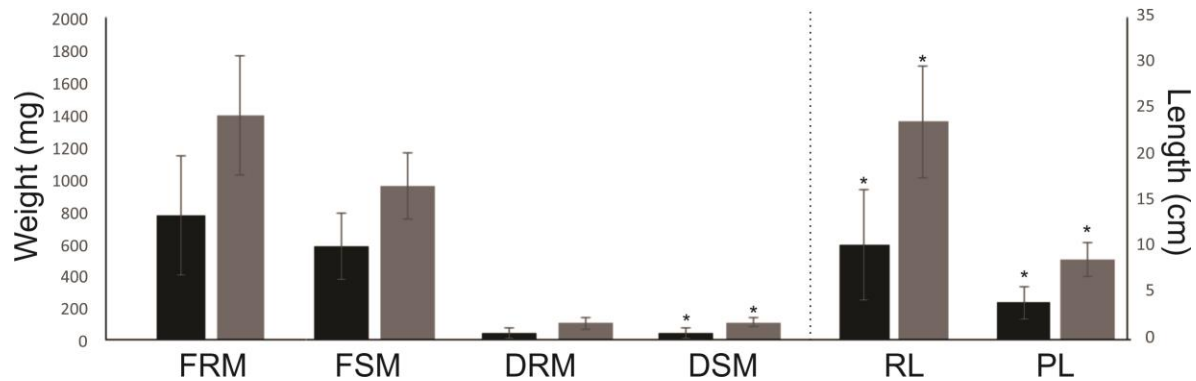
Figure 2: Biosynthesis of indole compounds in the presence and absence of Trp. An aliquot of the SMU inoculum was transferred to Dygs medium with or without tryptophan ($100 \text{ mg}\cdot\text{L}^{-1}$) and incubated for 72 h in the dark, at $30 \text{ }^\circ\text{C}$ and 150 rpm. To evaluate indole synthesis, $150 \text{ }\mu\text{L}$ of grown bacteria were transferred to microplates and $100 \text{ }\mu\text{L}$ of Salkowski reagent (see methods for details) were added. The plate was incubated for 30 min in the dark and samples analyzed at 492 nm on a spectrophotometer.



939
940
941
942
943
944
945
946
947
948

Figure 3: Dual growth assays of SMU and two phytopathogenic *Fusarium* species. Controls were conducted with *F. oxysporum* and *F. solani* grown without SMU (a and d, respectively). In the dual growth assays, SMU was placed in four equidistant regions to the *F. oxysporum* and *F. solani* (b and e, respectively). The adherence of SMU to *F. oxysporum* and *F. solani* hyphae was demonstrated by optical microscopy (c and f, respectively).

949



950

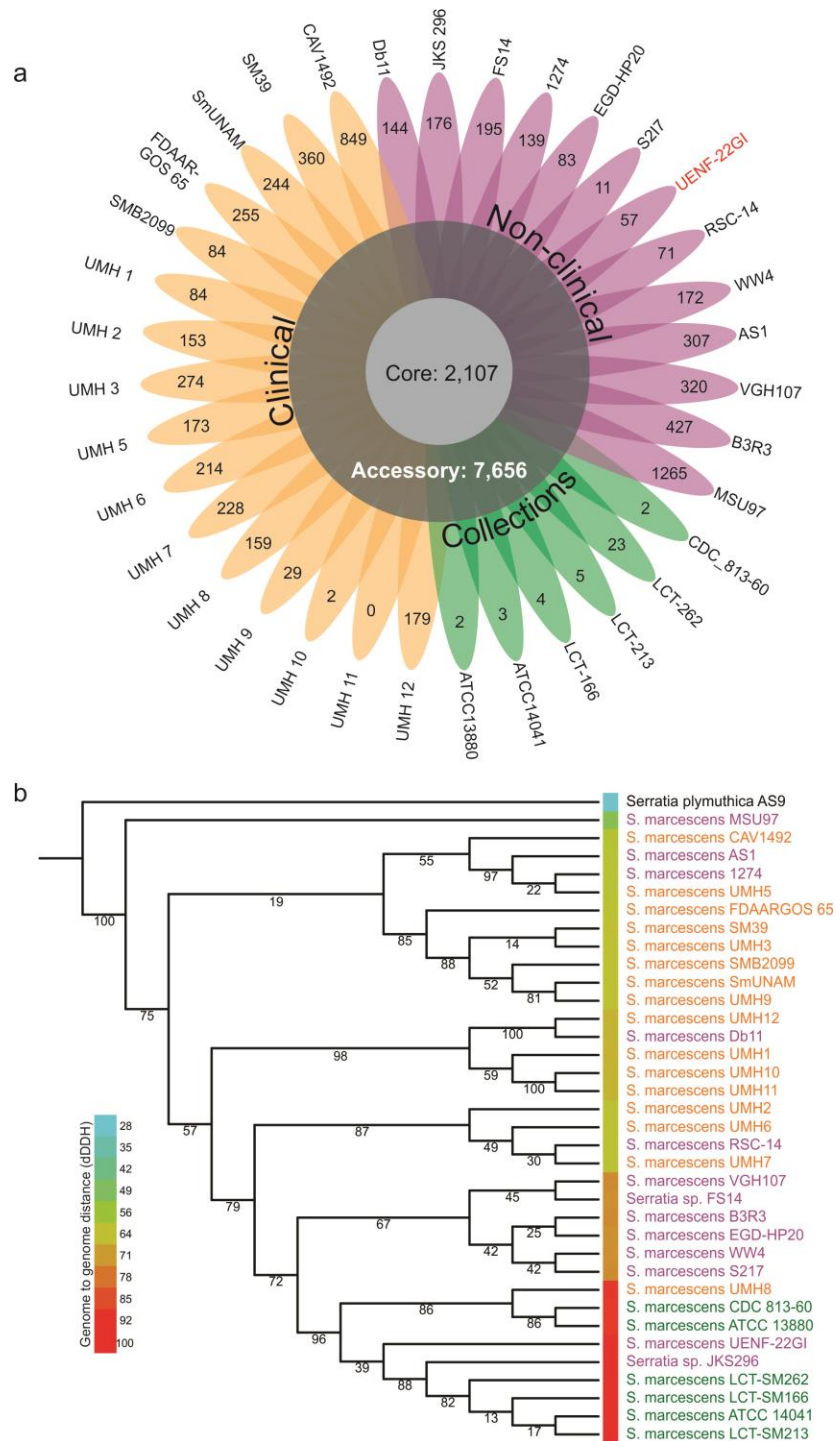
951

952

953

954 **Figure 4:** Effect of SMU inoculation on maize seedlings. Germinated seedlings (with 2 to 2.5 cm radicle
955 root length) were transferred to glass tubes containing sterilized vermiculite (one seed per tube).
956 Inoculation was performed by application of 1 mL of the SMU suspension (10^8 cells·mL⁻¹) over the
957 seedlings (gray bars). Plants inoculated with 1 mL of the sterile Dygs medium were used as negative
958 controls (black bars). The following metrics were recorded after 10 days: Fresh root mass (FRM), fresh
959 shoot mass (FSM), dry root mass (DRM), dry shoot mass (DSM), root length (RL) and plant height.
960 Experiments were conducted in triplicates and statistical significance assessed by a by Tukey test ($p <$
961 0.05).

962

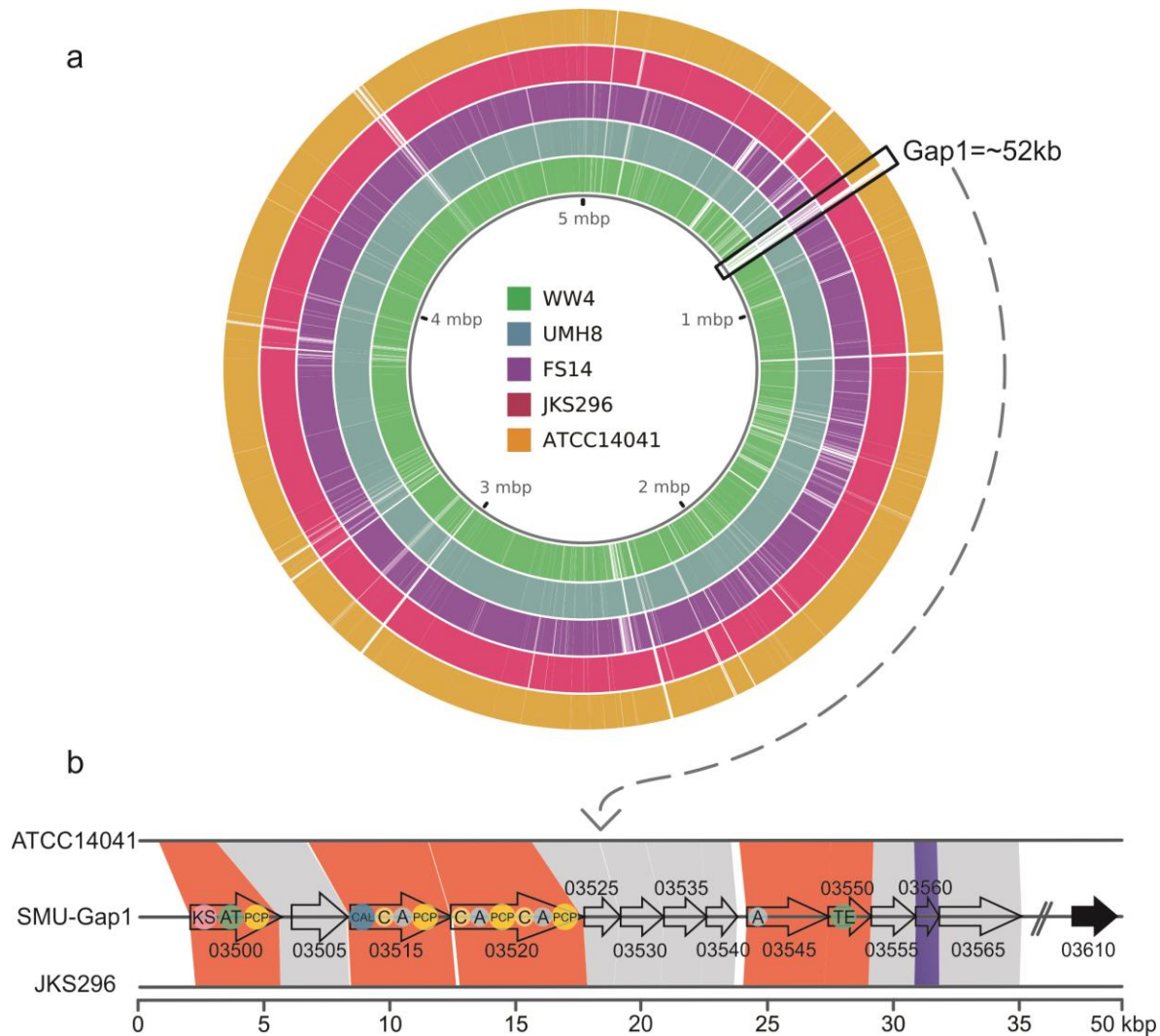


963

964

965 **Figure 5:** (a) Pan-genome of 35 *S. marcescens* isolates represented as a flowerplot. Clinical, non-clinical
 966 and collection *S. marcescens* isolates are represented in yellow, pink and green, respectively. Labels on
 967 petal tips represent strain-specific genes. (b) Multi-locus maximum likelihood tree reconstructed using
 968 concatenated alignment of 10 single-copy core genes. Branch labels represent bootstrap support (in
 969 percentage; 1000 bootstrap replicates). The blue-to-red heatmap accounts for the distance of each
 970 isolate to SMU, estimated by the digital DNA:DNA hybridization (dDDH) method.

971
972



973
974
975
976
977
978
979
980
981
982
983
984

Figure 6: (a) Whole-genome alignment of SMU and some of the closest reference genomes. The black box indicates the horizontally-acquired region (Gap1); (b) Synteny analysis of part of the genes within Gap1 region, emphasizing the presence of the NRPS-PKS domains: KS (ketosynthase), AT (acyltransferase), PCP (peptidyl carrier domain), CAL (coenzyme A ligase), C (condensation), A (adenylation) and TE (thioesterase). AK961_03560 encodes an antitoxin protein. AK961_03610 encodes an integrase that likely delimits the end of Gap1.

985 **Table 1:** SMU genes associated with plant-growth promotion features discussed in this study.

Phosphate and zinc solubilization	
Annotation entry (AK961_)	Protein name
07090, 07095, 07100, 07105, 07110	pqqB, pqqC, pqqD, pqqE, pqqF
10840	(PQQ)-dependent glucose dehydrogenase
17880	gluconolactonase
08395	2-gluconate dehydrogenase
17580, 17575, 17570	2-keto-gluconate dehydrogenase
21125, 21130, 21135, 21140, 21145	phoU, pstB, pstA, pstC, pstS
Tolerance against metal toxicity	
01055	Arsenate reductase
03990	ArsR family transcriptional regulator of arsRBC operon
03995	arsB arsenical pump membrane protein
04000	arsC1 arsenate reductase
01905, 01915	Copper resistance protein
09290	Copper resistance protein copD
07435, 07440	Chromate transporter
12615	Cobalt-zinc-cadmium efflux system
IAA and spermidine-related	
01575	ipdC
00655, 12310	Auxin efflux carrier
18130, 18125	speAB
18275, 18270	speDE
Biofilm formation	
20475, 20470, 20465, 20460, 20480, 20485	bcsA, bcsB, bcsC, bcsZ bcsQ, bcsR
20490, 20495, 20500	bcsE, bcsF, bcsG
01650, 01655, 1660, 01665	pgaA, pgaB, pgaC, pgaD
13115	adrA
Biocontrol and resistance	
20530, 01270, 12935, 05475	chiA, chiB, chiD, chiA1
13300, 13305, 13310, 13315, 13320, 13325, 13330, 13335, 13340, 13345, 13350, 13355, 13360, 13365	pigA, pigB, pigC, pigD, pigE, pigF, pigG, pigH, pigI, pigJ, pigK, pigL, pigM, pigN
16235	Kasugamycin resistance protein ksgA
03740, 14040	Bicyclomycin resistance protein
02590	Bicyclomycin multidrug efflux system
13395	Fosmidomycin resistance protein
07380	Barnase inhibitor
08005	Fusaric acid resistance protein